



# The Aarhus Chamber Campaign on Highly Oxygenated Organic Molecules and Aerosols (ACCHA): particle formation, organic acids, and dimer esters from $\alpha$ -pinene ozonolysis at different temperatures

Kasper Kristensen<sup>1</sup>, Louise N. Jensen<sup>2</sup>, Lauriane L. J. Quéléver<sup>3</sup>, Sigurd Christiansen<sup>2</sup>, Bernadette Rosati<sup>2,4</sup>, Jonas Elm<sup>2</sup>, Ricky Teiwes<sup>4</sup>, Henrik B. Pedersen<sup>4</sup>, Marianne Glasius<sup>2</sup>, Mikael Ehn<sup>3</sup>, and Merete Bilde<sup>2</sup>

<sup>1</sup>Department of Engineering, Aarhus University, 8000 Aarhus C, Denmark

<sup>2</sup>Department of Chemistry and iCLIMATE, Aarhus University, 8000 Aarhus C, Denmark

<sup>3</sup>Institute for Atmospheric and Earth System Research – INAR/Physics, University of Helsinki, P.O. Box 64, 00014, Helsinki, Finland

<sup>4</sup>Department of Physics and Astronomy, Aarhus University, 8000 Aarhus C, Denmark

**Correspondence:** Kasper Kristensen (kasper.kristensen@eng.au.dk) and Merete Bilde (bilde@chem.au.dk)

Received: 4 February 2020 – Discussion started: 10 February 2020

Revised: 13 August 2020 – Accepted: 14 August 2020 – Published: 2 November 2020

**Abstract.** Little is known about the effects of subzero temperatures on the formation of secondary organic aerosol (SOA) from  $\alpha$ -pinene. In the current work, ozone-initiated oxidation of  $\alpha$ -pinene at initial concentrations of 10 and 50 ppb, respectively, is performed at temperatures of 20, 0, and  $-15^\circ\text{C}$  in the Aarhus University Research on Aerosol (AURA) smog chamber during the Aarhus Chamber Campaign on Highly Oxygenated Organic Molecules and Aerosols (ACCHA). Herein, we show how temperature influences the formation and chemical composition of  $\alpha$ -pinene-derived SOA with a specific focus on the formation of organic acids and dimer esters. With respect to particle formation, the results show significant increase in particle-formation rates, particle number concentrations, and particle mass concentrations at low temperatures. In particular, the number concentrations of sub-10 nm particles were significantly increased at the lower 0 and  $-15^\circ\text{C}$  temperatures. Temperature also affects the chemical composition of formed SOA. Here, detailed offline chemical analyses show that organic acids contribute from 15 % to 30 % by mass, with highest contributions observed at the lowest temperatures, indicative of enhanced condensation of these semivolatile species. In comparison, a total of 30 identified dimer esters were seen to contribute between 4 % and 11 % to the total SOA mass. No significant differences in the chemical composition

(i.e. organic acids and dimer esters) of the  $\alpha$ -pinene-derived SOA particles are observed between experiments performed at 10 and 50 ppb initial  $\alpha$ -pinene concentrations, thus suggesting a higher influence of reaction temperature compared to that of  $\alpha$ -pinene loading on the SOA chemical composition. Interestingly, the effect of temperature on the formation of dimer esters differs between the individual species. The formation of less oxidized dimer esters – with oxygen-to-carbon ratio (O : C)  $< 0.4$  – is shown to increase at low temperatures, while the formation of the more oxidized species (O : C  $> 0.4$ ) is suppressed, consequently resulting in temperature-modulated composition of the  $\alpha$ -pinene-derived SOA. Temperature ramping experiments exposing  $\alpha$ -pinene-derived SOA to changing temperatures (heating and cooling) reveal that the chemical composition of the SOA with respect to dimer esters is governed almost solely by the temperature at which oxidization started and is unsusceptible to subsequent changes in temperature. Similarly, the resulting SOA mass concentrations were found to be more influenced by the initial  $\alpha$ -pinene oxidation temperatures, thus suggesting that the formation conditions to a large extent govern the type of SOA formed, rather than the conditions to which the SOA is later exposed.

For the first time, we discuss the relation between the identified dimer ester and the highly oxygenated or-

ganic molecules (HOMs) measured by chemical ionization–atmospheric pressure interface–time-of-flight mass spectrometer (CI-API-ToF) during the ACCHA experiments. We propose that, although very different in chemical structures and O : C ratios, many dimer esters and HOMs may be linked through similar RO<sub>2</sub> reaction pathways and that dimer esters and HOMs merely represent two different fates of the RO<sub>2</sub> radicals.

## 1 Introduction

The oxidation of volatile organic compounds (VOCs) constitutes an important source of secondary organic aerosol (SOA) in the atmosphere. Due to its atmospheric reactivity and its high estimated global emission rate of  $\sim 30 \text{ Tg yr}^{-1}$  (Sindelarova et al., 2014), the atmospheric oxidation of the biogenic VOC  $\alpha$ -pinene has been widely studied. The boreal forests are considered abundant sources of  $\alpha$ -pinene, with varying but sizeable emissions occurring all year round (Hakola et al., 2003, 2009; Noe et al., 2012). In addition, Lee et al. (2020) and Zhang et al. (2018) show that monoterpene-originated SOA are the largest sources of particulate matter in the southeastern US. For this reason, the oxidation of  $\alpha$ -pinene and subsequent formation of SOA is expected to occur at conditions with a wide range of VOC concentrations and atmospheric temperatures.

A number of smog chamber studies have investigated the effect of  $\alpha$ -pinene concentration and reaction temperature on the formation of SOA from  $\alpha$ -pinene oxidation (Svendby et al., 2008; Pathak et al., 2007; Tillmann et al., 2010; Warren et al., 2009; Kourtchev et al., 2016; Kristensen et al., 2017; Zhao et al., 2019a). Most of published studies, however, focus on SOA mass yield (defined as mass of SOA formed per mass of reacted VOC) and report higher yields with increasing VOC concentrations and lower temperatures. The effect of subzero temperatures, on gas-phase oxidation products, nucleation, particle growth and particle chemical composition, remains a largely unexplored area (Huang et al., 2018; Stolzenburg et al., 2018).

Once emitted to the atmosphere,  $\alpha$ -pinene is oxidized through reactions with atmospheric oxidants such as ozone (O<sub>3</sub>), hydroxyl (OH<sup>•</sup>), and nitrate (NO<sub>3</sub><sup>•</sup>) radicals. These reactions have been shown to result in numerous oxidation products with various chemical functionalities, including alcohols, aldehydes, ketones, carboxylic acids, peroxides, and peroxy acids (Nizkorodov et al., 2011; Noziere et al., 2015). As a result of their lower volatilities, many  $\alpha$ -pinene-derived oxidation products (e.g. carboxylic acids) partition to already existing particles in the atmosphere, contributing to particle growth and increasing SOA mass. The extent and timescale at which an organic compound undergoes partitioning is related to its saturation vapour pressure, the available particle mass (Kroll and Seinfeld, 2008), and particle size and par-

ticle phase (Shiraiwa and Seinfeld, 2012; Li and Shiraiwa, 2019; Zaveri et al., 2014, 2020). Due to the temperature dependence of the saturation vapour pressures of organic oxidation products, higher SOA mass yields from increased condensation of organics have been observed at lower temperatures (Pathak et al., 2007; Saathoff et al., 2009; Warren et al., 2009; Svendby et al., 2008). The saturation vapour pressure of a given organic species is closely related to its chemical structure. Depending on their specific molecular structure and the amount of strong hydrogen bond donor–acceptor groups, the products of  $\alpha$ -pinene oxidation may undergo condensation or, with sufficiently low volatility, nucleation, with the latter resulting in new particle formation (Kulmala et al., 2013; Riccobono et al., 2014).

In addition to temperature-dependent condensation of oxidation products, temperature-modulated gas and multiphase chemistry have been suggested to influence SOA yields from VOC oxidation. The work of von Hessberg et al. (2009) observed oscillatory positive temperature dependence under dry conditions and suggested that SOA yields from  $\beta$ -pinene oxidation are governed to a higher degree by the temperature and humidity dependence of the involved chemical reactions than by vapour pressure of the formed oxidation products at different temperatures. Furthermore, Pathak et al. (2007) observed that  $\alpha$ -pinene SOA yields showed a weak dependence on temperature in the 15 to 40 °C range, implying that the negative temperature dependence of the partitioning is counteracted by a positive dependence of the chemical reaction mechanism. Multiple studies report on new particle formation arising from the oxidation of  $\alpha$ -pinene and suggest the formation of so-called extremely low volatility organic compounds (ELVOC; Donahue et al., 2012b) capable of gas-to-particle conversion (Bonn and Moorgat, 2002; Lee and Kamens, 2005; Gao et al., 2010; Tolocka et al., 2006; Claeys et al., 2009; Ehn et al., 2014; Metzger et al., 2010; Kirkby et al., 2016; Bianchi et al., 2019). Although the chemical composition of  $\alpha$ -pinene SOA has been extensively studied, uncertainty still remains regarding the chemical structure and functional groups of the compounds responsible for nucleation. Recent quantum chemical results indicate that multicarboxylic acids with three or more acid moieties are some of the most likely compounds to participate in new particle formation (Elm et al., 2017, 2019). In relation, Lawler et al. (2018) observed enhanced content of alkanolic acids in newly formed 20–70 nm particles in the Finnish boreal forest.

Recently, highly oxygenated organic molecules (HOMs) have been identified in  $\alpha$ -pinene oxidation studies (Bianchi et al., 2019; Ehn et al., 2014; Jokinen et al., 2014; Rissanen et al., 2015). Formed via a gas-phase autoxidation reaction (Crouse et al., 2013) involving intramolecular hydrogen abstraction by peroxy radicals, HOMs represent a class of organic compounds which can promptly reach high degrees of oxygenation (Ehn et al., 2017). Oxygen-to-carbon (O : C) ratios exceeding unity have been reported for monomer com-

pounds (Mutzel et al., 2015; Ehn et al., 2014). The high O : C ratios are attributed to multiple hydroperoxide functionalities, and the compounds have been perceived as likely candidates for nucleation and initial particle growth owing to their low volatilities (Tröstl et al., 2016; Kirkby et al., 2016). However, computational studies have shown that HOMs originating from  $\alpha$ -pinene autoxidation can have surprisingly high vapour pressures considering their oxidation state, and it is mainly the dimeric compounds that are likely to be classified as ELVOC (Kurteín et al., 2016; Peräkylä et al., 2020).

High-molecular-weight (MW > 300 Da) dimer esters formed from oxidation of  $\alpha$ -pinene have been identified in laboratory-generated and ambient air SOA (Hoffmann et al., 1998; Tolocka et al., 2004; Gao et al., 2004; Yasmeen et al., 2010; Witkowski and Gierczak, 2014; Kourtchev et al., 2015; Zhang et al., 2015; Kristensen et al., 2013, 2014, 2016, 2017; Mohr et al., 2017). Several mechanisms for the formation of dimer esters have been proposed, including gas-phase mechanisms such as clustering of carboxylic acids (Hoffmann et al., 1998; Claeys et al., 2009a; DePalma et al., 2013) and reactions involving reactive intermediate radicals such as stabilized Criegee intermediates (sCI) and RO<sub>2</sub> species (Kristensen et al., 2016; Zhang et al., 2015; Berndt et al., 2016; Witkowski and Gierczak, 2014; Zhao et al., 2015; Kahnt et al., 2018).

The high abundance of dimer esters detected in freshly formed  $\alpha$ -pinene-derived SOA particles (Kristensen et al., 2016) suggests that these compounds may be important for the initial formation and growth of atmospheric particles – a hypothesis supported by saturation vapour pressure estimates reported in Kristensen et al. (2017) classifying dimer esters as ELVOC with vapour pressures suitable for gas-to-particle phase conversion at room temperatures. Furthermore, recent studies show that dimer esters and other oligomeric compounds in atmospheric aerosol are strongly correlated with cloud condensation nuclei activity, thus suggesting a significant impact on climate (Kourtchev et al., 2016).

In contrast to dimer esters, few studies have identified particle-phase HOMs, and thus their fate upon gas–particle partitioning remains elusive. Recently, Zhang et al. (2017) identified highly oxidized monomers (C<sub>8–10</sub>H<sub>12–18</sub>O<sub>4–9</sub>) and dimers (C<sub>16–20</sub>H<sub>24–36</sub>O<sub>8–14</sub>) in  $\alpha$ -pinene-derived SOA particles using Na<sup>+</sup> attachment during electrospray ionization. The dimers identified by Zhang et al. (2017) show a somewhat different chemical formula and degree of oxidation than the gas-phase HOM dimers previously identified by Ehn et al. (2014), where the observed dimer composition was C<sub>19–20</sub>H<sub>28–32</sub>O<sub>11–18</sub>. This can be attributed to decomposition of the hydroperoxide functionality of HOMs from processes such as photolysis, thermolysis, and solvation, yielding alkoxy radicals, esters, and other moieties. The chemical formulas of the dimeric compounds in Zhang et al. (2017) show good resemblance to the dimer esters published in Kristensen et al. (2016), characterized as C<sub>15–19</sub>H<sub>24–30</sub>O<sub>5–10</sub>. This raises the important question of how different types

of identified dimers, including HOMs and dimer esters, are related via gas–particle partitioning, chemical reactions, or other processes.

The Aarhus Chamber Campaign on Highly Oxygenated Organic Molecules and Aerosols (ACCHA) presented in this work was designed to elucidate the formation of HOMs and dimer esters from the dark ozonolysis of  $\alpha$ -pinene at different temperatures. The effect of temperature and  $\alpha$ -pinene concentration on SOA formation and composition on the formation of HOMs and dimer esters is investigated through a series of chamber experiments at temperatures prevailing at the latitudes of the boreal forests (Hakola et al., 2009), i.e. from 20 to  $-15$  °C.

The results of ACCHA are presented in multiple publications. The elemental composition of the bulk  $\alpha$ -pinene SOA by high-resolution time-of-flight aerosol mass spectrometer (HR-ToF-AMS) is reported in the companion paper by Jensen et al. (2020). A study presenting factor analysis of proton transfer (PTR)-ToF-MS data includes a case study from the ACCHA campaign (Rosati et al., 2019). The formation of gas-phase HOMs as measured by nitric-acid-based chemical ionization–atmospheric pressure interface–time-of-flight (CI-API-ToF) mass spectrometer is presented in the work by Quéléver et al. (2019).

In the current work, we present the effect of temperature and  $\alpha$ -pinene concentrations on the formation and molecular composition of SOA particles formed from ozone-initiated oxidation of  $\alpha$ -pinene. Specifically, we investigate the contributions of organic acids and dimer esters to  $\alpha$ -pinene SOA formed at temperatures of 20, 0, and  $-15$  °C and examine the changes in molecular composition arising from heating and cooling of SOA particles.

## 2 Method

### 2.1 Chamber experiments

Dark ozonolysis of  $\alpha$ -pinene was conducted in the Aarhus University Research on Aerosol (AURA) smog chamber. The chamber is described in detail in Kristensen et al. (2017). In short, the AURA chamber consists of a 5 m<sup>3</sup> Teflon bag situated in a 27 m<sup>3</sup> temperature-controlled cold room. The chamber temperature can be varied from  $-16$  to  $+26$  °C. The temperature and relative humidity (RH) are monitored in the centre of the Teflon bag by a HC02 probe coupled to a HygroFlex HF320 transmitter (Rotronic AG, Switzerland). Additional instrumentations are situated in air-conditioned (at constant 20 °C) laboratory surrounding the cold room. In the current study, the chamber was operated using dry purified air (active carbon, HEPA) at atmospheric pressure. Ozone (O<sub>3</sub>;  $\sim 100$  ppb) was added to the chamber using an ozone generator (model 610, Jelight Company, Inc.), and the concentrations of O<sub>3</sub> and oxides of nitrogen (NO and NO<sub>2</sub>) were monitored by UV photometric (O342 Module, Environ-

ment S.A.) and chemiluminescent monitors (AC32M, Environment S.A.), respectively. A known amount of VOC was added to a 10 mL glass manifold, evaporated, and transferred to the chamber through a stainless-steel inlet (diameter = 10 mm; length = 100 cm) using heated (70 °C) N<sub>2</sub> flow. The concentration of the added VOC was monitored using a gas chromatograph with flame ionization detector (Agilent 7820A GC-FID, with a time resolution of 6 min) and a proton transfer reaction–time-of-flight mass spectrometer (PTR-ToF-MS 8000; IONICON, Innsbruck, Austria) sampling through stainless-steel outlets located opposite the VOC inlet (distance between inlet and outlet: ~ 1.6 m). Particle size distributions were measured using a scanning mobility particle sizer (SMPS) system including a Kr-85 neutralizer (TSI 3077A) and an electrostatic classifier (TSI 3082) coupled with a nano water-based condensation particle counter (CPC; TSI 3788). The SMPS system was optimized for measurements of particles in the range of 10–400 nm with a sampling time of 80 s (60 s upscan; 20 s downscan; aerosol flow rate = 1.6 L min<sup>-1</sup>; sheath flow rate = 5 L min<sup>-1</sup>). In addition, the total particle number concentration of particles with diameter ( $D_p$ ) larger than ~ 1.4 nm was measured by a particle size magnifier (PSM; A10, Airmodus; Vanhanen et al., 2011; sample flow = 2.5 L min<sup>-1</sup>; time resolution = 1 s) operated in fixed saturator flow mode. SMPS and PSM measurements were performed as close as possible to the cold-room trough with insulated tubing extending ~ 40 and ~ 10 cm from the cold room, respectively, thus minimizing residence time and potential influences caused by temperature variations.

The chemical composition of gas-phase HOMs was measured using a nitric-acid-based chemical ionization–atmospheric pressure interface–time-of-flight mass spectrometer (CI-APi-TOF; Tofwerk A.G., Switzerland, and Aerodyne Research Inc., USA) as presented by Junninen et al. (2010) and Jokinen et al. (2012). An Aerodyne high-resolution time-of-flight aerosol mass spectrometer (HR-ToF-AMS, Aerodyne Research Inc.; DeCarlo et al., 2006) was deployed to measure real-time, nonrefractory particulate matter. In addition, SOA molecular composition with respect to organic acids and high-molecular-weight dimer esters was investigated through offline filter analysis of the formed  $\alpha$ -pinene-derived SOA performed using an ultrahigh-performance liquid chromatograph coupled to the electrospray ionization source of a Bruker Daltonics quadrupole time-of-flight mass spectrometer (UHPLC/ESI-qToF-MS). Filter sampling was performed when no additional growth in SOA mass was evident from the SMPS and no  $\alpha$ -pinene could be detected by the GC-FID. All filter samples were collected by a low-volume sampler onto 47 mm and 0.20  $\mu$ m PTFE filters (Advantec) situated in stainless-steel filter holders at a flow rate of ~ 27 L min<sup>-1</sup>. After collection, the filter samples were stored at –20 °C until extraction and analysis.

A total of 12  $\alpha$ -pinene oxidation experiments conducted in the AURA smog chamber are presented here (Table 1). Each experiment was performed at temperatures close to

20, 0, or –15 °C to investigate the effect of temperature on the formation and composition of both gas- and particle-phase organics from dark ozonolysis of  $\alpha$ -pinene. Five experiments were conducted with the injection of 10 ppb  $\alpha$ -pinene (~ 0.32  $\mu$ L; 99 %, Sigma Aldrich; Exp. 1.1–1.5) into the ozone-filled chamber (~ 100 ppb O<sub>3</sub>). These experiments include oxidation at constant temperatures 20, 0, and –15 °C (Exp. 1.1, 1.2, and 1.3) and two temperature-ramp experiments (Exp. 1.4 and 1.5). The ramp experiments were performed by injection of  $\alpha$ -pinene at a fixed 20 °C (Exp. 1.4) or –15 °C (Exp. 1.5) temperature followed by subsequent ramping to –15 or 20 °C, respectively. In both experiments the gradual and continuous temperature ramping was initiated approximately 40 min after the injection of  $\alpha$ -pinene, hence before the SOA mass formation plateaued. In Exp. 1.4 a decrease in temperature from 20 to –15 °C was achieved in ~ 100 min, while in Exp. 1.5, heating of the chamber from –15 to 20 °C was performed in ~ 140 min. Note that small variations in RH (< 25 %) are observed in between all conducted experiments arising from heating or cooling of the dry chamber air (Table 1).

To investigate the effect of  $\alpha$ -pinene concentration on the SOA formation and composition, three experiments were performed with 50 ppb of  $\alpha$ -pinene (~ 1.6  $\mu$ L, 99 %, Sigma Aldrich) at 20, 0, and –15 °C (Exp. 2.1–2.3) and repeated (Exp. 2.3b and Exp. 3.1–3.3). All experiments were performed without the addition of an OH scavenger to the chamber.

Throughout this paper SOA density is assumed to be 1 g cm<sup>-3</sup> as in Kristensen et al. (2017).

## 2.2 Offline particle analysis by UHPLC/ESI-qToF-MS

Collected particle filter samples were extracted and analysed for organic acids and dimer esters. Filter extraction was performed using a 1 : 1 mixture of methanol and acetonitrile (HPLC grade, Sigma Aldrich), and 0.2  $\mu$ g of camphoric acid recovery standard was added to the filter sample prior to the addition of the extraction mixture to minimize uncertainties related to the offline extraction and analysis. The samples were placed in a cooled ultrasonic bath for 15 min; after which the filters were removed, and the extracts were filtered through a Teflon filter (0.45  $\mu$ m pore size, Chromafil). The extraction solvents were then removed by evaporation over gentle N<sub>2</sub> flow, and the residues were dissolved by adding 0.2 mL Milli-Q water with 10 % acetonitrile and 0.1 % acetic acid. The reconstituted samples were placed in a cooled ultrasonic bath for 5 min and the extract transferred to a HPLC sample vial for analysis. To ensure complete transfer of organics from the evaporated extracts, additional reconstitutions were performed with 0.2 mL Milli-Q water with 50 % acetonitrile and 0.1 % acetic acid. Both sample solutions (10 % and 50 % acetonitrile reconstitution) were analysed by UHPLC/ESI-qToF-MS immediately after extraction.

**Table 1.** Overview of conducted  $\alpha$ -pinene ozonolysis experiments. NA – not available

ID	Date	Exp. type	$\alpha$ -Pinene (ppb)	Ozone (at injection) (ppb)	Temp. <sup>a</sup> (at injection) (°C)	RH <sup>a</sup> (at injection) (%)	Temp. avg. <sup>b</sup> (°C)	RH avg. <sup>b</sup> (%)	VOC loss rate <sup>c</sup> (h <sup>-1</sup> )	Max. SOA mass <sup>d</sup> ( $\mu\text{g m}^{-3}$ )	Max. particle number <sup>d</sup> (10–400 nm) (no. cm <sup>-3</sup> )	Max. particle number (> 1.4 nm) (no. cm <sup>-3</sup> ) <sup>e</sup>
1.1	20161202	Low load, 20 °C	10	104	20.2	0	20.3 ( $\pm 0.1$ )	0.8 ( $\pm 0.8$ )	NA	6	3.9 $\times 10^4$	5.2 $\times 10^4$
1.2	20161208	Low load, 0 °C	10	105	0.9	2.9	0.7 ( $\pm 2.7$ )	7.1 ( $\pm 4.1$ )	NA	9	7.9 $\times 10^4$	17.0 $\times 10^4$
1.3	20161207	Low load, -15 °C	10	106	-13.7	8	-14.7 ( $\pm 0.1$ )	12.9 ( $\pm 5.3$ )	NA	15	7.4 $\times 10^4$	19.5 $\times 10^4$
1.4	20161209	Low load, 20 to -15 °C	10	103	19.9	0	NA	NA	NA	8	4.4 $\times 10^4$	8.4 $\times 10^4$
1.5	20161220	Low load, -15 to 20 °C	10	113	-14	11.7	5.3 ( $\pm 4.0$ )	5.3 ( $\pm 4.0$ )	NA	10	9.4 $\times 10^4$	20.0 $\times 10^4$
2.1 <sup>g</sup>	20161212	High load, 20 °C	50	105	19.8	0	20 ( $\pm 1.1$ )	1.1 ( $\pm 1.3$ )	1.0	50	8.2 $\times 10^4$	11.0 $\times 10^4$
2.2	20161219	High load, 0 °C	50	107	-0.4	6.9	-0.3 ( $\pm 0.1$ )	6.9 ( $\pm 0.8$ )	0.9	65	19.0 $\times 10^4$	> 70.0 $\times 10^4$ <sup>f</sup>
2.3a	20161213	High load, -15 °C	50	101	-13.1	6.7	-14.9 ( $\pm 0.6$ )	11.9 ( $\pm 4.3$ )	0.8	120	24.0 $\times 10^4$	> 70.0 $\times 10^4$ <sup>f</sup>
2.3b <sup>g</sup>	20161221	High load, -15 °C	50	113	-14.0	19.8	-15.0 ( $\pm 0.2$ )	24.7 ( $\pm 3.6$ )	0.8	131	16.0 $\times 10^4$	51.2 $\times 10^4$
3.1	20170112	High load, 20 °C	50	100	20.3	0	20.1 ( $\pm 0.5$ )	2.4 ( $\pm 2.0$ )	1.1	50	7.8 $\times 10^4$	8.4 $\times 10^4$
3.2	20170116	High load, 0 °C	50	105	0.2	8.6	0.0 ( $\pm 0.1$ )	8.7 ( $\pm 1.1$ )	1.0	78	25.0 $\times 10^4$	> 70.0 $\times 10^4$ <sup>f</sup>
3.3	20170113	High load, -15 °C	50	105	-14.5	11.2	-14.8 ( $\pm 0.6$ )	15.8 ( $\pm 4.5$ )	0.9	115	23.0 $\times 10^4$	> 70.0 $\times 10^4$ <sup>f</sup>

<sup>a</sup> Temperature and RH measured in centre of Teflon bag. <sup>b</sup> Average temperature and RH ( $\pm$ SD) were measured over the entire experiment. <sup>c</sup> VOC loss rates are estimated from GC-FID measurements.

<sup>d</sup> Measured by SMPS (10–400 nm). <sup>e</sup> Measured by PSM (> 1.4 nm). <sup>f</sup> PSM overloaded. <sup>g</sup> Temperature ramps were performed after the stable temperature phase and are presented in Jensen et al. (2020).

The HPLC stationary phase was a Waters ACQUITY UPLC ethylene bridged hybrid C18 column (2.1  $\times$  100 mm 1.7  $\mu\text{m}$ ), while the mobile phase consisted of acetic acid 0.1 % (*v/v*) in Milli-Q water (eluent A) and acetic acid 0.1 % (*v/v*) in acetonitrile as eluent B. The operating conditions of the mass spectrometer have been described elsewhere (Kristensen and Glasius, 2011).

Quantification of the organic acids was performed from eight-level calibration curves (0.1 to 10.0  $\mu\text{g mL}^{-1}$ ) of the following acids: cis-pinic, cis-pinonic acid, terpenylic acid, diaterpenylic acid acetate (DTAA), and 3-methyl-butane tri-carboxylic acid (MBTCA). The analytical uncertainty is estimated to be < 20 % for carboxylic acids. Due to lack of authentic standards, the dimer esters were quantified using DTAA as surrogate standard. DTAA was chosen due to its structural similarities with that of the dimer esters (dicarboxylic acid with ester functionality) as well as similar UH-PLC retention time.

### 3 Results and discussions

A representative example of the results obtained from the conducted smog chamber experiments is shown in Fig. 1. Following injection of  $\alpha$ -pinene into the ozone-filled chamber at constant temperature and RH, rapid particle formation is captured by the PSM (measuring particles > 1.4 nm) and, shortly after, the SMPS (10–400 nm). In all conducted experiments, maximum particle number concentrations were obtained within 10 min after  $\alpha$ -pinene injection followed by decay ascribed to wall loss and particle aggregation. Particle number concentrations shown in Fig. 1 (lower panel) are wall-loss corrected. During the course of the experiment, decrease in ozone and  $\alpha$ -pinene concentration is accompanied by increase in particle SOA mass concentration as measured by the SMPS. Figure 1 (upper panel) shows the wall-loss-corrected SOA mass concentration obtained from ozone-initiated oxidation of 50 ppb  $\alpha$ -pinene (measured by GC-FID). Wall-loss corrections were based on first-order fits to the SOA mass or number concentration after peak. The grey shaded area represents the time of filter sampling for offline chemical analysis by UHPLC/ESI-qToF-MS. Similar figures showing data from all conducted experiments are presented in the Supplement.

#### 3.1 Particle-formation rates and SOA mass yields

Figure 2a–b show the total particle number concentration (no. cm<sup>-3</sup>) as measured by the PSM ( $D_p > 1.4$  nm) at 20, 0, and -15 °C as a function of time after injection of 10 and 50 ppb  $\alpha$ -pinene, respectively. The maximum total particle number concentrations in all experiments are listed in Table 1. Particle formation in terms of number concentrations from the dark ozonolysis of  $\alpha$ -pinene at both 10 and 50 ppb VOC concentrations shows negative dependence on temper-

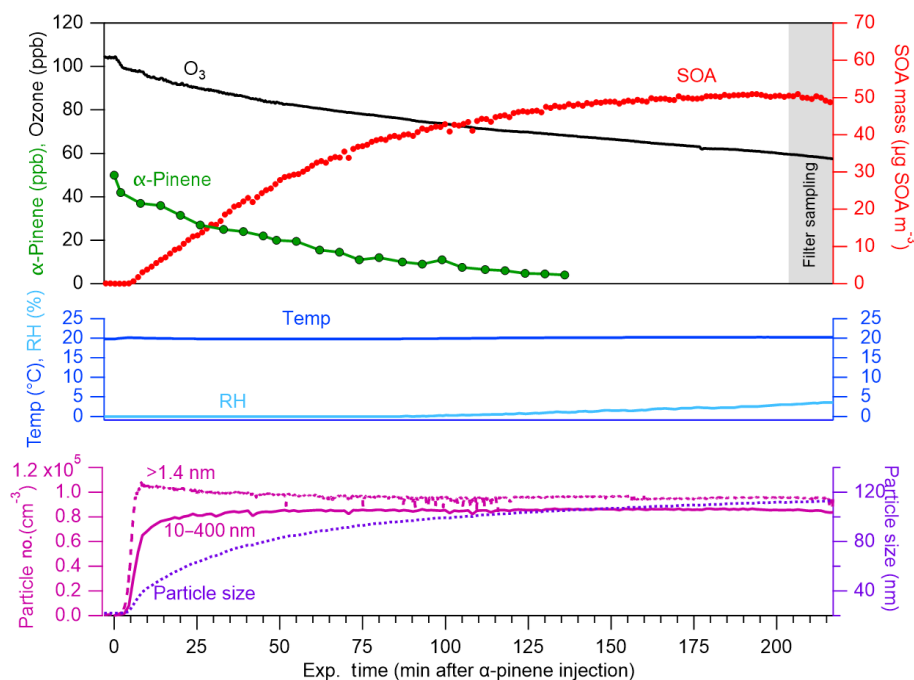


**Figure 1.** Concentration of  $O_3$  (ppb; black),  $\alpha$ -pinene (ppb; green), wall-loss-corrected SOA mass ( $\mu\text{g m}^{-3}$ ; red) and particle number concentration ( $\text{no. cm}^{-3}$ ; measured by PSM, for  $> 1.4 \text{ nm}$ , and SMPS, for 10–400 nm; dark red), and the geometric mean particle size (nm; by SMPS; violet) along with recorded RH (%) and temperature ( $^{\circ}\text{C}$ ; blue) during a 50 ppb  $\alpha$ -pinene oxidation experiment performed at  $20^{\circ}\text{C}$  (Exp. 2.1).

ature as has also been reported previously (Jonsson et al., 2008; Kristensen et al., 2017). Maximum particle-formation rates ( $\text{no. cm}^{-3} \text{ s}^{-1}$ ) are estimated from linear fits to the experimental time series of total particle number concentration measured by the PSM (Fig. 2a–b). Due to inhomogeneous mixing in the beginning of the experiments (when the particle formation is most efficient) as well as uncertainties related to the PSM cut-off, the presented particle-formation rates should be considered rough estimates and likely not accurate formation rates of e.g. 2 nm particles. However, it is clear that lower temperatures result in relatively higher particle-formation rates from ozone-initiated oxidation of  $\alpha$ -pinene at both low (10 ppb) and high (50 ppb) VOC concentrations. At both  $\alpha$ -pinene concentrations, a significantly higher particle-formation rate is observed when oxidation takes place at  $0^{\circ}\text{C}$  compared to oxidation performed at  $20^{\circ}\text{C}$ , with the formation rates being  $\sim 6$  times and  $\sim 20$  times higher at 0 than at  $20^{\circ}\text{C}$ , at 10 and 50 ppb  $\alpha$ -pinene experiments, respectively. In comparison, the maximum particle-formation rate at both  $\alpha$ -pinene concentrations only increased by a factor of 1.5 when performing the oxidation at  $-15^{\circ}\text{C}$  compared to  $0^{\circ}\text{C}$ .

Figure 2c–d show the evolution of the wall-loss-corrected SOA mass concentration ( $\mu\text{g m}^{-3}$ ) measured by SMPS as a function of time after  $\alpha$ -pinene injection. Agreeing with previous studies, SOA mass and mass yields are higher at lower temperatures (Jonsson et al., 2008; Saathoff et al., 2009; Pathak et al., 2007; Kristensen et al., 2017). The reported

18 % and 43 % mass yields at 20 and  $-15^{\circ}\text{C}$ , respectively (50 ppb  $\alpha$ -pinene, 100 ppb  $O_3$ ), are in excellent agreement with previous values of 21 % and 39 % from similar oxidation experiments (50 ppb  $\alpha$ -pinene; 200 ppb  $O_3$ ) performed under similar conditions in the AURA chamber (Kristensen et al., 2017). Compared to experiments performed at  $20^{\circ}\text{C}$ , temperatures of 0 and  $-15^{\circ}\text{C}$ , respectively, result in  $\sim 50$  % and  $\sim 150$  % higher SOA mass concentrations. Interestingly, SOA mass concentration in both 10 and 50 ppb  $\alpha$ -pinene oxidation experiments show almost identical response to temperature going from reaction temperatures of 20 to  $-15^{\circ}\text{C}$ . In Fig. 2c and d, the maximum SOA mass is obtained faster at higher reaction temperatures than at lower temperatures. For both low (10 ppb) and high (50 ppb)  $\alpha$ -pinene concentrations, maximum SOA mass is reached approximately 140, 200, and 250 min after  $\alpha$ -pinene injection at 20, 0, and  $-15^{\circ}\text{C}$ , respectively. This is attributed to the faster reaction of  $\alpha$ -pinene with ozone at higher temperatures, which is also evident from the calculated  $\alpha$ -pinene loss rates shown in the inset in Fig. 2d (50 ppb; GC-FID derived; due to the detection limit of the GC-FID no loss rates could be calculated for 10 ppb  $\alpha$ -pinene experiments). Compared to oxidation experiments performed at  $20^{\circ}\text{C}$ , loss rates of  $\alpha$ -pinene were found to be 11 % and 22 % lower at 0 and  $-15^{\circ}\text{C}$  reaction temperature, respectively. These results are in good agreement with temperature-dependent reaction rates of ozone with  $\alpha$ -pinene reported by Atkinson et al. (1982) predicting a 16 ( $\pm 4$ ) %

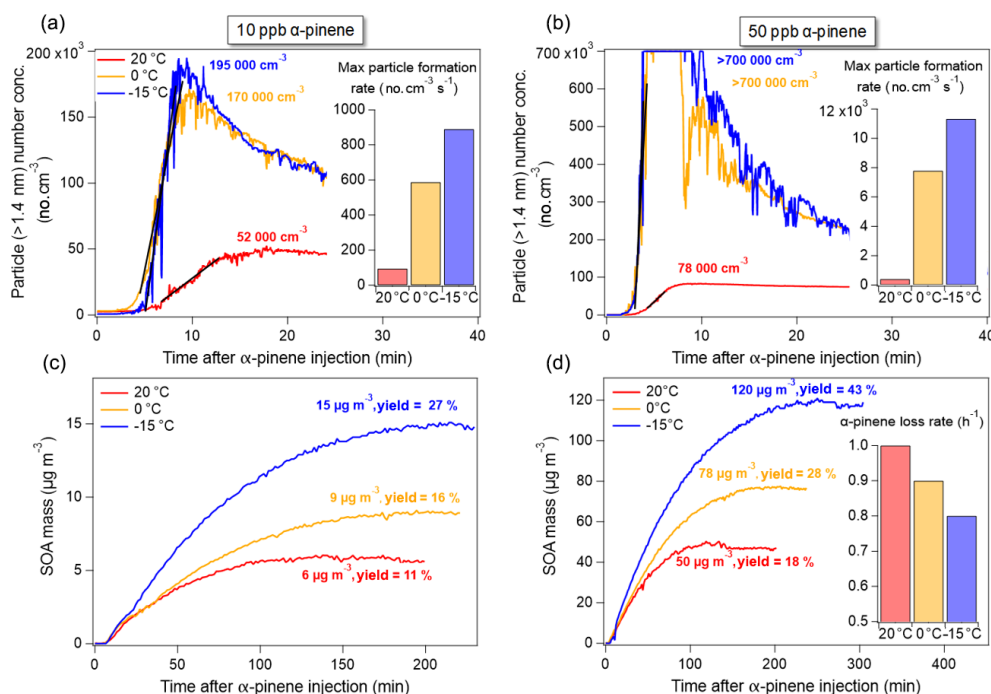


**Figure 2.** Effect of reaction temperature and initial VOC concentration on SOA formation with respect to (a, b) particle number concentration and (c, d) wall-loss-corrected SOA mass concentration at  $\alpha$ -pinene concentrations of (a, c) 10 ppb and (b, d) 50 ppb. Insets show particle-formation rates ( $\text{no. cm}^{-3} \text{s}^{-1}$ ) as estimated from linear fits to the (a, b) experimental data. The inset in (d) shows the loss rate of  $\alpha$ -pinene ( $\text{h}^{-1}$ ) at different temperatures as derived from an exponential fit to the measured concentration of  $\alpha$ -pinene.

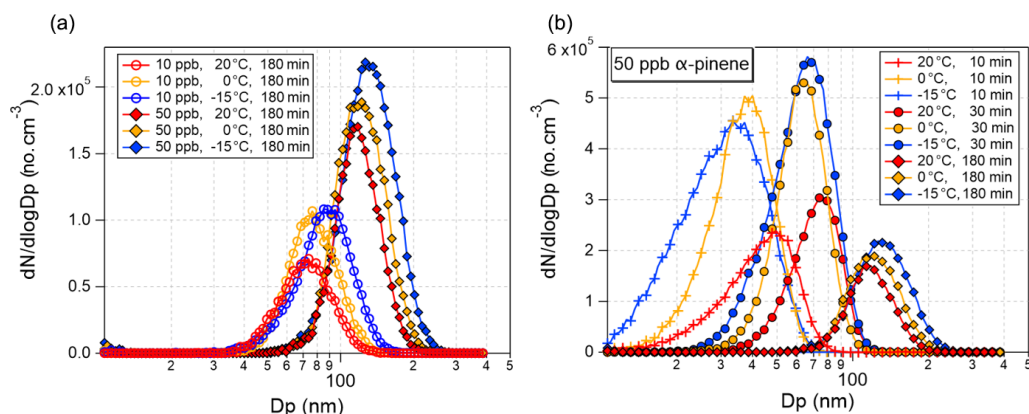
and 28 ( $\pm 6$ ) % lower reaction rate at 0 and  $-15^{\circ}\text{C}$ , respectively, relative to the reaction rate calculated at  $20^{\circ}\text{C}$ . The discrepancy between measured and literature-derived values is likely due to the presence of OH radicals in the current study. Despite the lower reaction rate for  $\alpha$ -pinene ozonolysis at low temperature, the particle number concentrations data, in Fig. 2, show significantly faster particle formation in cold experiments.

### 3.2 Particle size distributions and sub-10 nm particles

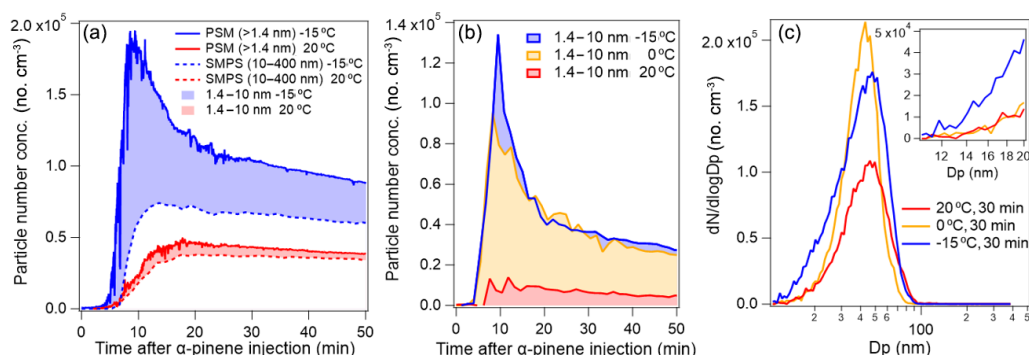
Figure 3a shows the particle size distributions as recorded by the SMPS after the maximum SOA mass concentration was reached in low (10 ppb)- and high (50 ppb)-concentration  $\alpha$ -pinene oxidation experiments at 20, 0, and  $-15^{\circ}\text{C}$ . At both  $\alpha$ -pinene concentrations, lower reaction temperatures result in larger particles consistent with the higher SOA masses at 0 and  $-15^{\circ}\text{C}$  in Fig. 3c and d. The time evolutions of the particle size distribution (Fig. 3b) shows that particles formed at  $20^{\circ}\text{C}$  are initially larger than the particles formed at the two lower temperatures (0 and  $-15^{\circ}\text{C}$ ). However, during the course of the experiments, particles formed at the lower temperatures grow more rapidly to larger sizes compared to particles formed at  $20^{\circ}\text{C}$ . This is likely attributable to enhanced condensation of organics onto the formed particles at lower temperatures.

Figure 4a shows the total particle number concentration ( $\text{no. cm}^{-3}$ ) obtained by the PSM ( $D_p > 1.4 \text{ nm}$ ) and SMPS ( $D_p$  in the range 10–400 nm), respectively, as a function of time after  $\alpha$ -pinene injection (10 ppb) at both 20 and  $-15^{\circ}\text{C}$ . The differences in the total particle number concentrations derived by the two instruments correspond to the number concentrations in the size range of 1.4 to 10 nm. Comparing experiments performed at 20, 0, and  $-15^{\circ}\text{C}$  temperatures in Fig. 4b (10 ppb  $\alpha$ -pinene), it is clear that the presence of sub-10 nm particles is higher at low reaction temperatures and that the largest temperature dependence is in the range 20 to  $0^{\circ}\text{C}$ .

According to Fig. 4a, sub-10 nm particles constitute  $\sim 10\%$  and  $25\%$  of the total particle number concentration at 20 and  $-15^{\circ}\text{C}$ , respectively, even 30 min after  $\alpha$ -pinene injection where particle number concentrations have peaked. The size distributions obtained from the SMPS (Fig. 4c), however, indicate very few particles in the smaller size-ranges (i.e. below 20 nm; Fig. 4c inset) at this time of the experiments. A possible explanation for the high sub-10 nm particle number concentration is the presence of a particle distribution mode below the detectable range of the SMPS. Supporting this, Lee et al. (2016) reported an absence of particles in the size range between 3 and 8 nm in ambient air particle measurements (1–600 nm particle size distribution range combining PSM and SMPS data) during the Southern Oxidant and Aerosol Study (SOAS) field campaign. To our



**Figure 3.** (a) Particle size distribution recorded 180 min after the ozone-initiated oxidation of 10 (Exp. 1.1–1.3) and 50 ppb (Exp. 2.1–2.3)  $\alpha$ -pinene at 20 °C (red), 0 °C (orange), and –15 °C (blue). (b) Particle size distribution recorded 10, 30, and 180 min after injection of 50 ppb  $\alpha$ -pinene at 20 °C (Exp. 2.1, red), 0 °C (Exp. 2.2, orange), and –15 °C (Exp. 2.3, blue).



**Figure 4.** (a) Effect of temperature on particle number concentrations (no. cm<sup>-3</sup>) as derived from the SMPS (10–400 nm particle size range; broken line) and PSM (> 1.4 nm particle size range; solid line) in experiments with an initial  $\alpha$ -pinene concentration of 10 ppb. (Exp. 1.1, red; Exp. 1.3, blue). (b) Particle number concentrations (no. cm<sup>-3</sup>) of 1.4–10 nm particles in experiments with an initial  $\alpha$ -pinene concentration of 10 ppb performed at –15, 0, and 20 °C (Exp. 1.1, 1.2, and 1.3, respectively). (c) Particle size distributions recorded 30 min after the ozone-initiated oxidation of 10 ppb  $\alpha$ -pinene performed at 20 °C (red), 0 °C (orange), and –15 °C (blue) (Exp. 1.1–1.3).

knowledge, the current work represents the first indication of this observed “gap” in the particle size distribution in smog chamber experiments, thus emphasizing the need for further studies of sub-10 nm particle formation and detection from VOC oxidation.

### 3.3 Molecular composition

Figure 5 shows the detailed chemical composition of SOA with respect to organic acids and dimer esters at different temperatures (20, 0, and –15 °C) and at two different concentrations of  $\alpha$ -pinene (10 and 50 ppb, respectively). The acids and dimer esters identified are similar to those in Kristensen et al. (2017), where suggestions for molecular structures are given. From comparison of repeated experiments (Exp. 2.1–2.3 and Exp. 3.1–3.3), the uncertainties related to the presented UHPLC/ESI-qToF-MS results are estimated to be less than 10 % (Fig. S3 in the Supplement).

Significantly higher particle concentrations of  $\alpha$ -pinene-derived organic acids are evident at the lower, 0 and –15 °C, temperatures compared to 20 °C, supporting increased condensation of organics at lower temperatures. The total contributions of the identified acids to the formed SOA mass in experiments with an initial  $\alpha$ -pinene concentration of 10 ppb are 17 %, 25 %, and 32 % at 20, 0, and –15 °C, respectively. In comparison, in the 50 ppb  $\alpha$ -pinene oxidation experiments, the acids contribute to the formed SOA with 18 %, 38 %, and 28 %, respectively. For comparison, the fraction of acids was 20 % at 20 °C and 31 % at –15 °C of total SOA mass in experiments with 50 ppb of  $\alpha$ -pinene and 200 ppb of ozone (Kristensen et al., 2017). Comparing mass fractions of acids at 20 and –15 °C, the mass fraction seems to be highly dependent on temperature and much less dependent on VOC concentration or VOC : O<sub>3</sub> ratios.

In all experiments, pinic acid was found to be the dominant identified organic acid, constituting between 5 % and 9 % of the formed SOA mass, with highest contributions at

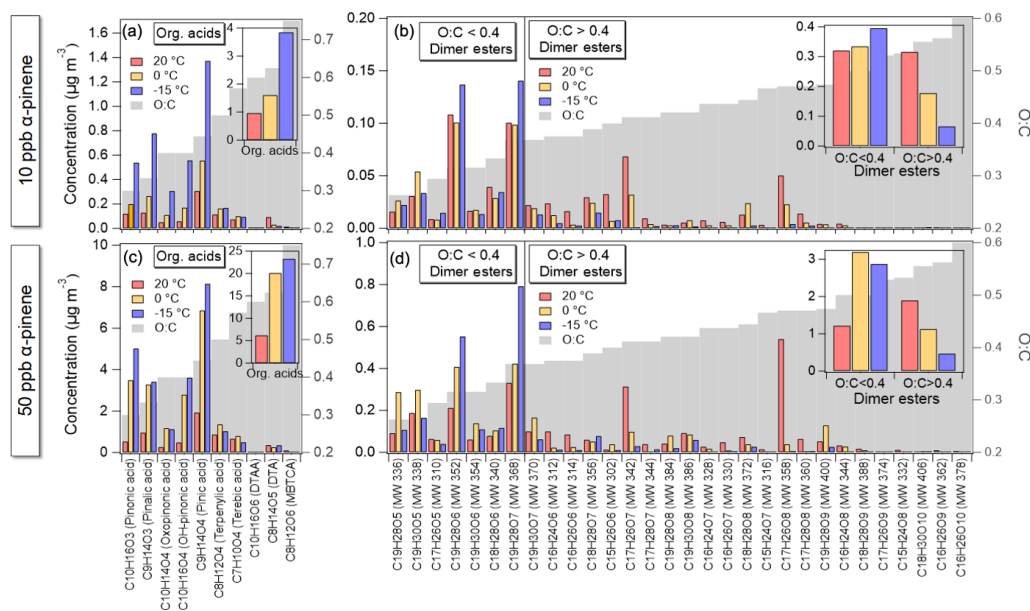


**Figure 5.** UHPLC/ESI-qToF-MS results showing mass concentrations ( $\mu\text{g m}^{-3}$ ; left axis) of acids and dimer esters as well as O : C ratios (grey bars, right axis) of these at 20 °C (red), 0 °C (orange), and -15 °C (blue) for the two  $\alpha$ -pinene concentrations: (a, b) 10 ppb and (c, d) 50 ppb. Insets show the total concentrations of the identified organic acids and dimer esters (O : C < 0.4 and O : C > 0.4).

lower reaction temperatures. A negative dependence of concentration with temperature is observed for 6 of the 10 identified organic acids: pinonic acid, pinalic acid, oxopinonic acid, OH-pinonic acid, pinic acid, and terpenylic acid. Di-terpenylic acid acetate (DTAA), di-terpenylic acid (DTA), and 3-methyl-butanetricarboxylic acid (MBTCA), however, show lower concentrations at the lower temperatures compared to at 20 °C. The effect of temperature seems to correlate with the O : C ratio (i.e. degree of oxidation of the organic acids) as shown in Fig. 5. Acids with lower O : C ratios (O : C < 0.4) are found at higher concentrations at lower temperatures (0 and -15 °C). This can likely be attributed to an enhanced condensation of these species onto the SOA particles at temperatures of 0 and -15 °C. In contrast, although contributing significantly less to the SOA mass, the more oxidized compounds (O : C > 0.4; DTAA, DTA and MBTCA) show an opposite trend with respect to temperature (Fig. S3). As MBTCA, DTAA, and DTA are hypothesized to be formed from gas-phase oxidations involving OH radicals (Szmigielski et al., 2007; Vereecken et al., 2007; Müller et al., 2012; Kristensen et al., 2014), their lower concentrations at lower reaction temperatures could be explained by (1) changes in reaction pathways or branching of the intermediates of MBTCA, DTAA, and DTA, (2) lower gas-phase concentration of the first generation of oxidized organic compounds due to a higher degree of condensation (e.g. MBTCA is formed from gas-phase oxidation of pinonic acid), and (3) reduction of OH radical production and hence reduced oxidation by OH radicals at lower reaction temperatures (Jonsson et al., 2008; Tillmann et al., 2010). The former (1) is sup-

ported by Müller et al. (2012) and Donahue et al. (2012a) reporting lower particle-phase MBTCA correlating with decreased pinonic acid vapour fractions at lower temperatures. Both explanations are supported by lower O : C ratios of the total  $\alpha$ -pinene-derived SOA formed at the lower temperatures as reported in Jensen et al. (2020).

A total of 30 dimer esters were identified in the collected SOA particle samples from both 10 and 50 ppb  $\alpha$ -pinene ozonolysis experiments. In the 10 ppb  $\alpha$ -pinene experiments, total concentrations of dimer esters of 0.64, 0.51, and 0.46  $\mu\text{g m}^{-3}$  were found in SOA particles formed at 20, 0, and -15 °C, respectively, thus showing a small positive dependence on temperature. The corresponding mass fractions were 11.1 %, 7.5 %, and 3.8 %. For particles formed from higher 50 ppb  $\alpha$ -pinene concentrations, the temperature dependence is less obvious, with total dimer ester concentration of 3.1, 4.3, and 3.3  $\mu\text{g m}^{-3}$  at 20, 0, and -15 °C, respectively. The corresponding mass fractions of the dimer esters are 8.9 %, 8.0 %, and 3.9 %, thus similar to fractions reported for the 10 ppb  $\alpha$ -pinene oxidation experiments – thus, as in the case of the organic acids, the mass fraction of dimer esters seems to be highly dependent on temperature and much less dependent on VOC concentrations or VOC : O<sub>3</sub> ratios. In relation, Kourtchev et al. (2016) observed a positive relationship between temperature and oligomer fraction in aerosol samples collected at Hyttiälä in summer 2011 and 2014 but ascribed this to differences in the VOC emissions. However, the current study, indicates that temperature alone may influence the aerosol fraction of dimeric compounds thus supporting the ambient observation in Kourtchev et al. (2016).

Looking at the concentrations of the 30 individual dimer esters identified in the current work, their formation is affected differently by the reaction temperature (Fig. 5). Figure 6a shows the yields of the identified dimer esters at  $-15^{\circ}\text{C}$  relative to  $20^{\circ}\text{C}$ ,  $\text{yield}(-15^{\circ}\text{C})/\text{yield}(20^{\circ}\text{C})$ , as a function of the number of carbon atoms in the dimer esters. From this, it is clear that the effect of temperature on the formation of individual dimer esters is compound specific. Of the 30 dimer esters, increased particle concentrations at lower temperatures is most often related to species with high carbon number (i.e.  $\text{C}_{19}$  species). Also, Fig. 6a shows that the temperature effect on the dimer ester concentration to a large extent depends on the O : C ratio (indicated by colour scale) of the individual species. This is highlighted also in Fig. 6b showing a more significant decrease in relative yields of dimer esters with higher oxygen number (i.e. more oxidized) at the lower  $-15^{\circ}\text{C}$  temperature in both 10 and 50 ppb  $\alpha$ -pinene experiments. Accordingly, the dimer esters are grouped based on their O : C ratios, with the more oxidized dimer esters having an O : C  $> 0.4$  – the O : C value above which all dimer esters show decreased concentration at the lower temperature of  $-15^{\circ}\text{C}$  compared to  $20^{\circ}\text{C}$  (Fig. S4). The total concentrations of the low ( $< 0.4$ )- and high ( $> 0.4$ )-O : C dimer esters are shown in Fig. 5b and d insets.

### 3.4 Temperature ramping

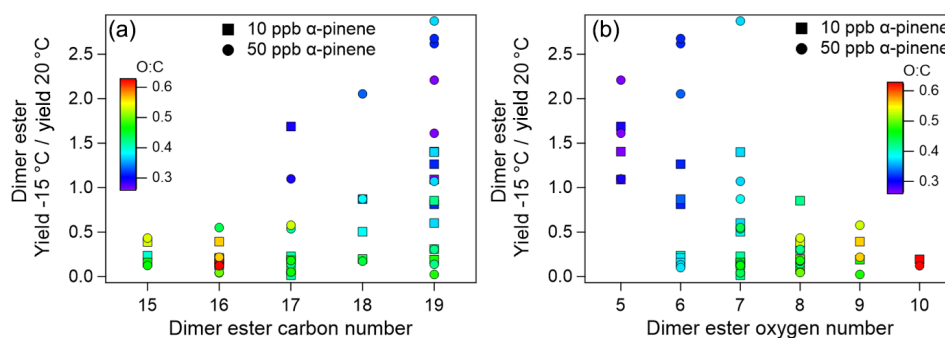
Normann Jensen et al. (2020) presented a detailed analysis on changes in AMS-derived elemental chemical composition during temperature ramps in the ACCHA campaign and showed that temperature at which the particles are formed to a large extent determines the elemental composition also after subsequent heating or cooling by  $35^{\circ}\text{C}$ . During two temperature-ramp experiments, we also studied how the concentration, mass fraction, and molar yields of carboxylic acids and dimer esters as identified in the offline analysis varied. The experiments involving temperature ramps were conducted to examine whether the observed effect of temperature on the dimer ester concentration is attributed to gas-to-particle partitioning or stabilization/decomposition of the hydroperoxide-containing species.

Figure 7a shows the SOA mass formation (wall-loss corrected) from the 10 ppb  $\alpha$ -pinene oxidation experiments performed at constant  $20^{\circ}\text{C}$  (Exp. 1.1) and  $-15^{\circ}\text{C}$  (Exp. 1.3) and from the two temperature ramping experiments (Exp. 1.4 and 1.5) in which the chamber temperature was ramped up or down  $\sim 40$  min after injection of  $\alpha$ -pinene. In the  $\sim 40$  min following the injection of  $\alpha$ -pinene, SOA mass in both ramp experiments show good agreement with the constant temperature experiments performed at similar starting temperature (Exp. 1.1 and 1.3). Likewise, particle-formation rates and maximum particle number concentrations obtained in Exp. 1.4 and 1.5 prior to temperature changes (Table 1) also resemble those of Exp. 1.1 and 1.3. Thus the initial evolution

of the particle formation in Exp. 1.1 (constant  $20^{\circ}\text{C}$ ) and Exp. 1.4 (ramp experiment initiated at  $20^{\circ}\text{C}$ ) and in Exp. 1.3 (constant  $-15^{\circ}\text{C}$ ) and Exp. 1.5 (ramp experiment initiated at  $-15^{\circ}\text{C}$ ) are comparable.

From Fig. 7a, cooling and heating the chamber imply a quasi-immediate effect on the SOA mass concentration. In Exp. 1.4, decreasing the temperature results in a maximum SOA mass concentration being  $\sim 30\%$  higher than the maximum SOA mass in Exp. 1.1 performed at a constant  $20^{\circ}\text{C}$  (8 versus  $6\mu\text{g m}^{-3}$ ). Conversely, heating the chamber from  $-15^{\circ}\text{C}$  to  $20^{\circ}\text{C}$  (Exp. 1.5) results in a  $\sim 30\%$  lower SOA mass (10 versus  $15\mu\text{g m}^{-3}$ ) compared to SOA formed and kept at  $-15^{\circ}\text{C}$  (Exp. 1.3). The changes in particle size distributions as a result of temperature ramping (Fig. 7b) are attributed to evaporation during heating and condensation during cooling. Interestingly, despite the loss or gain of particle mass during temperature ramping, the SOA mass concentration is closer to the experiments performed at the initial temperature rather than the final temperature even after a temperature ramp of  $35^{\circ}\text{C}$ . This, in turn, suggests that the formation conditions to a large extent govern the type of SOA that was formed, rather than the conditions the SOA was later exposed to.

Figure 8 shows the mass concentrations, mass fractions, and molar yields of organic acids and dimer esters in SOA particles from constant temperature oxidation experiments at 20 and  $-15^{\circ}\text{C}$  (Exp. 1.1 and 1.3, respectively) and from the two temperature-ramp experiments (Exp. 1.4 and 1.5). Upon heating SOA particles from  $-15$  to  $20^{\circ}\text{C}$ , a loss of particle mass ( $5\mu\text{g m}^{-3}$ ; Fig. 7) was observed and is attributed to evaporation of organics. This is supported by a  $2.8\mu\text{g m}^{-3}$  lower organic acid concentration in particles exposed to heating in Exp. 1.5 compared to particles formed at the constant  $-15^{\circ}\text{C}$  (Exp. 1.3), accounting for  $\sim 60\%$  of the evaporated organics. These results underline the semivolatile nature of the identified organic acids (i.e. pinalic acid, pinonic acid, oxopinonic acid, OH-pinonic acid, pinic acid, terpenylic acid, and terebic acid) and show that these acids are readily removed from organic aerosols during heating, thus explaining previously reported reduced aerosol mass fraction from heating  $\alpha$ -pinene SOA (Pathak et al., 2007). In contrast, cooling of the formed SOA particles in Exp. 1.4 resulted only in a small  $0.3\mu\text{g m}^{-3}$  increase in organic acid concentration, making up  $\sim 15\%$  of the reported  $2\mu\text{g m}^{-3}$  increase in SOA mass compared to the constant  $20^{\circ}\text{C}$  experiment. These results indicate limited gas-to-particle phase condensation of the semivolatile organic acids upon cooling the SOA. The current findings are in agreement with that of Zhao et al. (2019a), which found that during cooling of  $\alpha$ -pinene SOA particles, the resulting mass growth was largely over-predicted by the applied volatility basis set model. As suggested in Zhao et al. (2019a) the observed limited condensation of semivolatiles to SOA particles during cooling is likely attributed to an expected high particle viscosity at the relative low-RH conditions of the performed oxidation experiments.



**Figure 6.** Comparison of relative yields (yield at  $-15^{\circ}\text{C}$ /yield at  $20^{\circ}\text{C}$ ) for specific dimer esters as a function of dimer ester (a) carbon number and (b) oxygen number in 10 and 50 ppb  $\alpha$ -pinene ozonolysis experiments. Colour scale indicates the O : C ratio of the dimer esters.

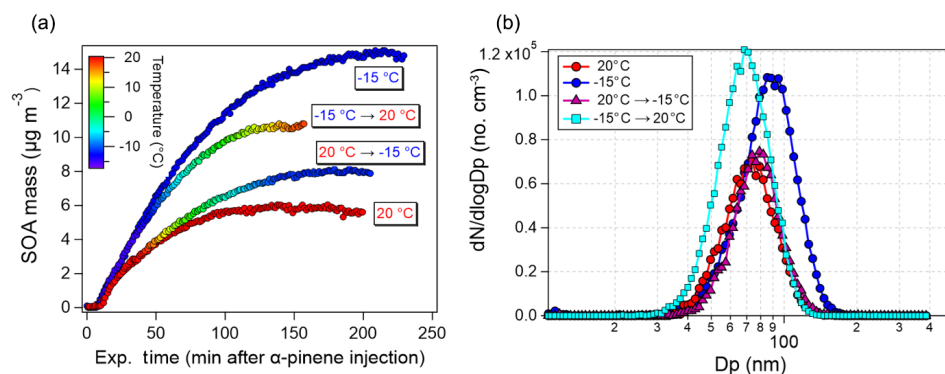


**Figure 7.** Effect of temperature ramping ( $20^{\circ}\text{C} \rightarrow -15^{\circ}\text{C}$ , Exp. 1.4, and  $-15^{\circ}\text{C} \rightarrow 20^{\circ}\text{C}$ , Exp. 1.5) on the (a) wall-loss-corrected SOA mass concentration and (b) final particle size distribution from ozonolysis of 10 ppb  $\alpha$ -pinene. For comparison, results from constant  $-15$  and  $20^{\circ}\text{C}$  temperature experiments (Exp. 1.1 and Exp. 1.3, respectively) are also shown.

Under these conditions, condensed SVOCs are likely confined to the near-particle-surface region, thus impeding further partitioning of the gas-phase SVOCs (Renbaum-Wolff et al., 2013). In the current study, this is supported by the relatively small increase in organic acids (Fig. 8) as well as almost negligible increase in particle size (Fig. 7b) observed upon cooling the SOA particles from  $20$  to  $-15^{\circ}\text{C}$ . Also, if SVOCs reside near the particle surface, this would indeed explain the effective evaporation of these compounds (i.e. the identified organic acids; Fig. 8) and subsequent reduction in particle size (Fig. 7b) observed in Exp. 1.5.

With respect to dimer esters, thermodynamics or partitioning could be considered as a possible explanation for the observed temperature responses of the high- and low-O : C dimer esters. As reported in Kristensen et al. (2017), the identified dimer esters span across a wide range of volatilities. Here, many of the low-O : C dimer esters may be sufficiently volatile to allow considerable fractions to exist in the gas phase at high temperatures. Consequently, the increased particle-phase concentration observed at the lower temperatures may solely be attributed to enhanced gas-to-particle phase partitioning of these species. Supporting this, Mohr et al. (2017) identified dimeric monoterpene oxidation prod-

ucts ( $\text{C}_{16-20}\text{H}_y\text{O}_{6-9}$ ) in both particle phase and gas phases in ambient air measurements in the boreal forest in Finland. However, Fig. 8 reveals that heating and cooling of  $\alpha$ -pinene-derived SOA particles, after their formation, results in insignificant or small changes in the concentrations, mass fractions, and molar yields of dimer esters when compared to experiments performed at constant temperatures. This indicates that the dimer esters are not subjected to evaporation or decomposition within the studied temperature range and timeframe. Also, the results indicate that the SOA particle dimer ester concentration is, within the timeframe of the performed experiments, unaffected by any changes to the particle phase state associated with either the performed cooling or heating of the particles. This could thus suggest that the formation of dimer esters proceed through gas-phase mechanism rather than reactions in the particle phase. Thus, the results show that the concentration of the dimer esters in SOA from  $\alpha$ -pinene oxidation is largely determined by the temperature at which the SOA is formed rather than subsequent exposure to higher or lower temperatures.

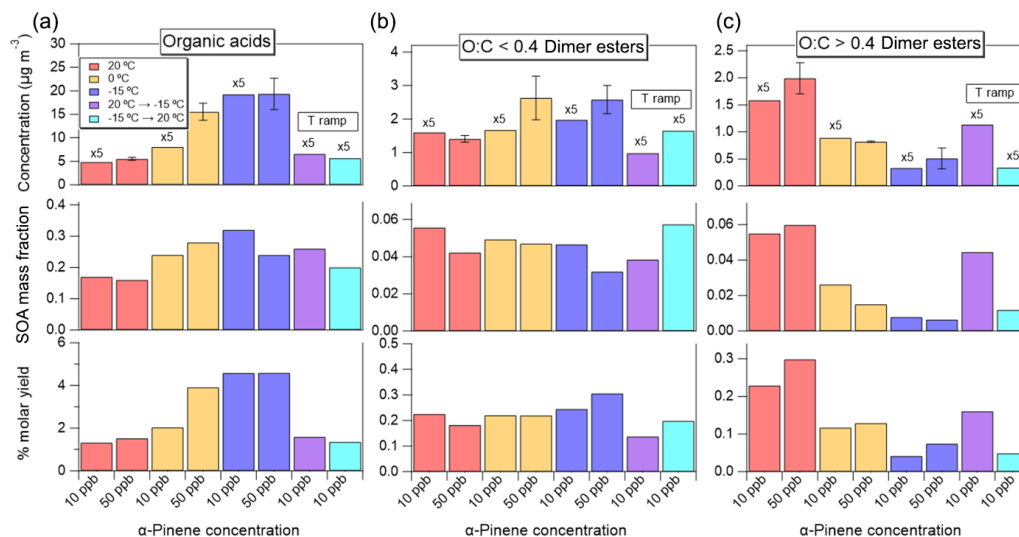


**Figure 8.** Effect of  $\alpha$ -pinene concentration and temperature on the mass concentrations ( $\mu\text{g m}^{-3}$ ), SOA mass fractions, and molar yield of the identified organic acids (column a), low-O : C ( $< 0.4$ ) dimer esters (column b), and high-O : C ( $> 0.4$ ) dimer esters (column c). Note that the concentrations ( $\mu\text{g m}^{-3}$ ) of organic acids and dimer esters related to the 10 ppb  $\alpha$ -pinene oxidation experiments have been multiplied with a factor of 5 (top panels). For the 50 ppb pinene oxidation experiments, average values are reported from Exp. 2.1–2.3 and Exp. 3.1–3.3. Error bars represent 1 standard deviation.

### 3.5 Dimer esters formation

Gas-phase formation of dimer esters from  $\alpha$ -pinene ozonolysis has been suggested to proceed through the reaction of stabilized Criegee intermediate (sCI) with carboxylic acids resulting in the formation of a class of ester hydroperoxides,  $\alpha$ -acyloxyalkyl hydroperoxides ( $\alpha$ -AAHPs) (Zhao et al., 2018a; Kristensen et al., 2016). In relation, Claffin et al. (2018) stated that the only known gas-phase mechanism for forming esters in their experiments was the reaction of sCI with carboxylic acids under dry conditions. As the reactions of sCI are expected to be temperature-dependent, this could explain the lower formation of some of the identified dimer esters (the high-O : C dimers) in the current study. Also, as suggested by Kristensen et al. (2017), temperature-modulated condensation of the gas-phase carboxylic acid precursors may also contribute to the observed temperature effects on the formation of dimer esters. As the condensation of the carboxylic acids is vapour pressure dependent, it is expected that the less volatile (i.e. more oxidized) species are more effectively depleted from the gas phase at lower temperatures, hence hindering their gas-phase reactions with the sCI and reducing formation of the more oxidized dimer esters. Consequently, at the lower temperatures the formation of dimer esters is more likely to proceed through reactions of sCI with the more volatile and less oxidized carboxylic acids species, thus potentially explaining the observed increased formation of the low-O : C dimer esters in the 0 and  $-15$  °C experiments. In addition to the observed temperature dependence of the low-O : C dimer esters, an increased stability

of hydroperoxide-containing species in SOA particles is expected at lower temperatures (Zhao et al., 2018a).

While the formation of  $\alpha$ -AAHPs through sCI and carboxylic acids is a plausible mechanism related to many of the dimer esters identified in the current study, this may not be true for all species. In particular, studies on the MW 368 dimer ester (pinonyl-pinyl ester,  $\text{C}_{19}\text{H}_{28}\text{O}_7$ ) and MW 358 (pinyl-diaterpenyl ester,  $\text{C}_{17}\text{H}_{26}\text{O}_8$ ) conclude that the chemical structures of these esters do not include hydroperoxide functionalities (Beck and Hoffmann, 2016; Kahnt et al., 2018). Consequently, Kahnt et al. (2018) recently suggested an alternative mechanism for the formation of these species involving gas-phase formation and subsequent rearrangement of unstable  $\text{C}_{19}\text{H}_{28}\text{O}_{11}$  HOM species formed from  $\text{RO}_2 + \text{R}'\text{O} \rightarrow \text{RO}_3\text{R}$  reaction of an acyl peroxy radical and an alkoxy radical. Specifically, Kahnt et al. (2018) explains that the  $\text{C}_{19}\text{H}_{28}\text{O}_{11}$  HOM species decompose through the loss of oxygen or ketene, resulting in the formation of the MW 368 dimer ester (pinonyl-pinyl ester,  $\text{C}_{19}\text{H}_{28}\text{O}_7$ ) and the MW 358 dimer ester (pinyl-diaterpenyl ester,  $\text{C}_{17}\text{H}_{26}\text{O}_8$ ), respectively. Interestingly, in the current study, the particle-phase concentration of the MW 368 dimer ester increases at lower temperatures, while the opposite is seen for the MW 358 dimer esters (Fig. 5), thus indicating significant differences in the mechanism responsible for the formation of these particular dimer esters. In accordance with the mechanism suggested by Kahnt et al. (2018), the different responses to temperature of the two dimer esters could be explained by (1) a temperature modulated formation of the alkoxy radicals related to the 5- and 7-hydroxy-pinonic acid involved in the formation of the two  $\text{C}_{19}\text{H}_{28}\text{O}_{11}$  HOM species decom-

posing to the MW 368 and MW 358 dimer esters, respectively, or (2) temperature-dependent decomposition and rearrangement of the  $C_{19}H_{28}O_{11}$  HOM species suppressing the more complex decomposition and rearrangement mechanism in which carbon-containing entities (e.g. ketene) are expelled from the HOM. However, these explanations are not supported by the temperature ramping experiments performed herein indicating that the formation of the dimer esters is determined by the initial reaction temperature and remains relatively unaffected by heating or cooling. In addition, although accounting for the differences in the temperature response of the MW 368 and MW 358 dimer esters – and to some extent the increased particle concentration of many higher carbon number dimer esters (i.e.  $C_{19}$  species; Fig. 6a) – a temperature-modulated decomposition does not solely explain the observed decrease in relative yields of dimer esters with higher oxygen number (Fig. 6b). To explain this, the formation and subsequent decomposition of more oxidized HOMs need to be considered as possible precursors for the more oxygen-rich dimer esters.

A detailed study on the formation of HOMs during the ACCHA campaign is presented by Quéléver et al. (2019). Here, significantly lower (by orders of magnitude) HOM gas-phase concentrations are observed in  $-15^{\circ}\text{C}$  experiments compared to  $20^{\circ}\text{C}$  experiments. As the HOMs form through autoxidation of  $\text{RO}_2$ , low temperatures – and thus decreased autoxidation – is expected to result in lower formation of HOMs with reduced formation of the more oxygenated species. Interestingly, however, Quéléver et al. (2019) observed no correlation between the degree of oxidation (i.e. O : C ratio) of the identified HOMs and the magnitude by which the formation of these was reduced at lower temperatures. This is in contrast to the observed temperature effects on the formation of the identified dimer esters presented in the current study (Fig. 7) and thus rules out the formation and decomposition of more oxidized HOMs as mechanism for the formation of more oxygen-rich dimer esters. In Quéléver et al. (2019), one possible interpretation of the observed temperature effect on HOMs is that the rate-limiting step in the autoxidation chain takes place already in the first steps of autoxidation. This is supported by the observed decreased concentration of dimer esters with a higher number of oxygen atoms, which also indicates that the formation of the identified dimer esters could proceed through reaction of products from  $\text{RO}_2$  autoxidation. The involved oxidation state of these products may vary depending on the degree of autoxidation undertaken by the  $\text{RO}_2$  radical as well as the radical termination of these, including unimolecular processes leading to loss of OH or  $\text{HO}_2$  or bimolecular reactions with NO,  $\text{HO}_2$ , or other  $\text{RO}_2$  resulting in the formation of ROOR dimers. As the autoxidation and the bimolecular reactions of  $\text{RO}_2$  radicals are temperature-dependent, these processes may provide explanation for the observed response to temperature of the different dimer esters. Claffin et al. (2018) showed that the autoxidation and radical termination reactions of the

Criegee intermediate  $\text{RO}_2$  radicals may result in a plethora of different products covering a range of oxidation states and functionalities – including multifunctional  $\text{RO}_2$  radicals, hydroperoxide, carbonyl, alcohol, carboxylic and peroxy-carboxylic acid, and dialkyl and diacyl peroxides. Of these, carbonyls, alcohols, and carboxylic acids react readily with sCI, resulting in dimeric compounds such as secondary ozonides,  $\alpha$ -alkoxyalkyl hydroperoxides (AAAHs), and  $\alpha$ -AAHP, respectively (Chhantyal-Pun et al., 2018; McGillen et al., 2017; Khan et al., 2018; Claffin et al., 2018). In relation,  $\text{RO}_2$ – $\text{RO}_2$  reactions have been proposed as conceivable mechanism for the formation of dimers from  $\alpha$ -pinene ozonolysis (Claffin et al., 2018; Zhao et al., 2018b). Here,  $\text{RO}_2$  produced from the isomerization or decomposition of Criegee intermediates are suggested to participate in  $\text{RO}_2$ – $\text{RO}_2$  reactions resulting in dialkyl or diacyl peroxides. The formation of dimer esters through reactions of  $\text{RO}_2$  is supported by an observed decrease in dimer esters concentrations at higher levels of  $\text{NO}_x$  in ambient air measurement in Hyytiälä, Finland (Kristensen et al., 2016) and supports the formation proposed by several studies (Ehn et al., 2014; Berndt et al., 2018; Zhao et al., 2018b) involving  $\text{RO}_2$  cross-reactions as likely route of gaseous dimer formation. The  $\text{RO}_2$ – $\text{RO}_2$  reaction is expected to compete with the reactions of  $\text{RO}_2$  with  $\text{HO}_2$  radicals. In the absence of an OH scavenger, the performed oxidation experiments will include the formation of OH radicals from the gas-phase reaction of  $\alpha$ -pinene with  $\text{O}_3$ . The formed OH radicals react readily with  $\text{O}_3$ , yielding  $\text{HO}_2$  radicals available for  $\text{RO}_2$ – $\text{HO}_2$  reactions. As both reactions ( $\text{O}_3 + \alpha$ -pinene and  $\text{O}_3 + \text{OH}$ ) have a positive temperature dependence, the formation of  $\text{HO}_2$  and its subsequent reaction with  $\text{RO}_2$  is expected to increase at the higher reaction temperatures. In Simon et al. (2020) the higher concentration of  $\text{HO}_2$  leads to an increased competition with the  $\text{RO}_2$ – $\text{RO}_2$  self-reaction, which reduced the formation of HOM dimers but increased HOM monomers. However, in the current study, reduction in the concentration of dimer esters due to increased  $\text{RO}_2$ – $\text{HO}_2$  competition at higher temperatures is only observed in the case of the low-O : C dimer esters, such as the pinonyl-pinyl ester. In the case of the higher-O : C dimers, it appears that a suppressed competition of  $\text{HO}_2$  with  $\text{RO}_2$  at the lower temperatures is less important and that other mechanisms are responsible for observed temperature effects on the more oxidized dimers.

Recently, heterogeneous chemistry has been suggested as a possible pathway for the formation of dimer ester in  $\beta$ -pinene oxidation experiments. Here, dimer esters are suggested to form from semivolatile dicarboxylic acids (e.g. pinic acid) undergoing traditional equilibrium gas–particle partitioning with subsequent reactive uptake of the gas-phase, OH-derived monomers on collision with particle surfaces to form dimer esters (Kenseth et al., 2018). In Kenseth et al. (2018), the suggested mechanism is supported by an observed increased formation of certain dimer esters in oxidation experiments including seed particles enriched with

pinic acid as well as an observed suppressed formation of some dimer esters in the presence of an OH scavenger. In relation, Zhao et al. (2019b) recently reported dimer formation through dimerization by organic radical (i.e., peroxy, RO<sub>2</sub>, and alkoxy radicals, RO) cross-reactions during heterogeneous OH-initiated oxidative ageing of oxygenated organic aerosol.

In the current study, heterogeneous chemistry and OH dependency could help explain the observed response to temperature of the identified dimer esters. At the lower, 0 and  $-15^{\circ}\text{C}$ , reaction temperatures increased condensation of semivolatile organic acids, such as pinic acid (Figs. 5 and 7), could facilitate the formation of dimer esters from these monomeric species. In addition, reduced OH radical production at lower reaction temperatures could explain the suppressed formation of the higher-O : C dimer esters from reduced formation of more oxidized organic species, such as MBTCA and DTAA (Fig. S3), and other OH-dependent monomers available for reactive uptake into the formed SOA particles or gas-phase reactions. This is somewhat supported by an observed correlations between the particle-phase concentration of pinic acid and the pinonyl-pinyl ester ( $R^2 = 0.92$ ; Fig. S6), whilst the more oxidized dimer ester pinyldiaterpenyl ester correlates better with MBTCA ( $R^2 = 0.99$ ; Fig. S6) rather than pinic acid ( $R^2 = 0.02$ ). Although correlation between particle-phase monomeric organic acids and dimer esters could suggest purely particle-phase chemistry as the mechanism for dimer ester formation, this is not supported by the relatively small changes in the dimer ester concentration following heating or cooling of the formed SOA particles (Fig. 8). In particular, temperature-ramping experiments show that while the particle-phase concentrations of pinic acid and MBTCA are affected by both heating and cooling of the SOA particles, both pinonyl-pinyl ester and pinyldiaterpenyl ester are unaffected, with concentrations determined by the initial reaction temperatures (Fig. S6). The observed temperature effects on dimer ester formation could be ascribed to oxidation by OH radicals of the dimer ester precursors, whether formed from autoxidation processes or RO<sub>2</sub> termination pathways, or to the dimer esters themselves, thus leading to the formation of high-O : C dimer esters.

We propose that, although different in chemical structures and O : C ratios, dimer esters and HOMs may be linked via their formation mechanisms, both involving RO<sub>2</sub>. The particle-phase dimer esters and the gas-phase HOMs may merely represent two different fates of the RO<sub>2</sub> radicals. If conditions are favourable and efficient autoxidation takes place, this will result in the formation of HOMs, which by the definition recommended by Bianchi et al. (2019) in this case means any molecule with six or more oxygen atoms that has undergone autoxidation. On the other hand, dimer esters could be the product of cross-reactions of RO<sub>2</sub> formed from autoxidation or formed from OH oxidation of the autoxidation termination products with O : C ratios influenced by the number of potential autoxidation steps undertaken by the in-

volved RO<sub>2</sub> species prior to reaction or termination. Whether the formation of dimer esters proceeds through gas-phase or heterogeneous RO<sub>2</sub>–RO<sub>2</sub> cross-reactions of species formed from autoxidation or from OH oxidation of termination products or through monomeric compounds reacting with sCI is yet to be determined.

#### 4 Conclusions

The formation of SOA from dark ozonolysis of  $\alpha$ -pinene is highly influenced by temperature. At subzero temperatures, such as  $-15^{\circ}\text{C}$ , more effective nucleation gives rise to significantly higher particle number concentration compared to similar experiments performed at  $20^{\circ}\text{C}$ , where the vast majority of laboratory studies are conducted. In addition, the SOA mass concentration resulting from  $\alpha$ -pinene ozonolysis shows a strong temperature dependence attributed to increased condensation of semivolatile oxidation products at lower temperatures. This is supported by higher concentration of semivolatile organic acids, such as pinic acid and pinonic acid, in SOA particles formed at  $0^{\circ}\text{C}$  and  $-15^{\circ}\text{C}$  compared to particles formed at  $20^{\circ}\text{C}$ . In addition to organic acids, the contribution of high-molecular-weight dimer esters to the formed SOA is also affected by temperature. Underlining the chemical complexity of  $\alpha$ -pinene SOA, the 30 quantified dimer esters showed different behaviours with respect to temperature, with the suppressed formation of the more oxidized dimer esters (O : C > 0.4) at low reaction temperatures. This feature is not seen in the case of the least oxidized dimer esters (O : C < 0.4), showing a small increase in particle concentration at lower temperatures. Similar to the high-O : C dimer ester compounds,  $\alpha$ -pinene ozonolysis experiments performed at lower temperatures result in lower HOM formation from autoxidation in the gas-phase. We suggest that the identified dimer esters may form through RO<sub>2</sub> cross-reactions with the oxidative state (i.e. O : C ratio) of the resulting dimer esters highly influenced by available OH radicals for the formation of more oxidized organic radicals prior to dimerization. Consequently, we speculate that the observed temperature effects on the identified dimer esters can be impacted by the OH formation and reactivity at the studied temperatures. These results indicate that temperature not only affects the formation of SOA mass in the atmosphere but also alters the chemical composition through condensation and evaporation of semivolatile species, changes in the formation of HOMs, and finally changes in the reaction pathways leading to the formation of dimer esters having high and low O : C ratios. With respect to dimer esters, no decomposition or evidence of partitioning changes between the aerosol and the gas phase was observed from heating or cooling the SOA particles, suggesting that (1) the formation and, consequently, concentration of dimer esters are dictated by the VOC oxidation conditions and (2) once formed, dimer esters remain in the particle phase, representing a core

compound within SOA and thus an efficient organic carbon binder to the aerosol phase. In relation, the presented results from temperature ramping show that final SOA mass concentration obtained from dark ozonolysis of  $\alpha$ -pinene is more dependent on the initial reaction temperatures rather than the temperatures to which the formed SOA is subsequently exposed. In conclusion, this means that the changes in ambient temperatures in areas of emissions and oxidation of VOCs, such as  $\alpha$ -pinene, are likely to result in significant changes to the resulting SOA mass as well as the chemical composition of the SOA. As global temperatures are expected to rise, especially in the Nordic regions of the boreal forests, this means that although less SOA mass is expected to form from the oxidation of emitted biogenic VOCs, the temperature-induced changes to the chemical composition may result in more temperature-resistant SOA influencing cloud-forming abilities from increased content of oligomeric compounds (i.e. dimer esters).

*Data availability.* Data related to this article are available upon request to the corresponding authors.

*Supplement.* The supplement related to this article is available online at: <https://doi.org/10.5194/acp-20-12549-2020-supplement>.

*Author contributions.* MB, ME, MG, and HBP supervised the AC-CHA campaign. KK, LLJQ, SC, ME, and MB designed the experiments. KK, LNJ, and SC initialized the chamber for experiments. KK and LNJ measured and analysed the aerosol phase. KK, BR, and RT measured and analysed the VOCs and their oxidation production. LLJQ performed the measurement and analysed the gas-phase HOMs. JE guided and helped with the interpretation of the dimer ester data and formation pathways. KK prepared the paper with the contributions from all co-authors.

*Competing interests.* The authors declare that they have no conflict of interest.

*Acknowledgements.* We thank Aarhus University and Aarhus University Research Foundation for support.

*Financial support.* This research has been supported by the Aarhus University Research Foundation, the European Research Council (grant no. 638703-COALA), and the Academy of Finland (grant nos. 307331, 317380, and 320094). Kasper Kristensen received financial support from the Carlsberg Foundation (grant no. CF18-0883). Jonas Elm received financial support from the Villum Foundation and the Swedish Research Council Formas (project number 2018-01745-COBACCA).

*Review statement.* This paper was edited by Manabu Shiraiwa and reviewed by two anonymous referees.

## References

- Atkinson, R., Winer, A. M., and Pitts, J. N.: Rate constants for the gas phase reactions of O<sub>3</sub> with the natural hydrocarbons isoprene and  $\alpha$ - and  $\beta$ -pinene, *Atmos. Environ.*, 16, 1017–1020, [https://doi.org/10.1016/0004-6981\(82\)90187-1](https://doi.org/10.1016/0004-6981(82)90187-1), 1982.
- Beck, M. and Hoffmann, T.: A detailed MSn study for the molecular identification of a dimer formed from oxidation of pinene, *Atmos. Environ.*, 130, 120–126, <https://doi.org/10.1016/j.atmosenv.2015.09.012>, 2016.
- Berndt, T., Richters, S., Jokinen, T., Hyttinen, N., Kurtén, T., Otkjær, R. V., Kjaergaard, H. G., Stratmann, F., Herrmann, H., and Sipilä, M.: Hydroxyl radical-induced formation of highly oxidized organic compounds, *Nat. Commun.*, 7, 13677, <https://doi.org/10.1038/ncomms13677>, 2016.
- Berndt, T., Scholz, W., Mentler, B., Fischer, L., Herrmann, H., Kulmala, M., and Hansel, A.: Accretion Product Formation from Self- and Cross-Reactions of RO<sub>2</sub> Radicals in the Atmosphere, *Angew. Chem. Int. Edit.*, 57, 3820–3824, <https://doi.org/10.1002/anie.201710989>, 2018.
- Bianchi, F., Kurtén, T., Riva, M., Mohr, C., Rissanen, M. P., Roldin, P., Berndt, T., Crouse, J. D., Wennberg, P. O., Mentel, T. F., Wildt, J., Junninen, H., Jokinen, T., Kulmala, M., Worsnop, D. R., Thornton, J. A., Donahue, N., Kjaergaard, H. G., and Ehn, M.: Highly Oxygenated Organic Molecules (HOM) from Gas-Phase Autoxidation Involving Peroxy Radicals: A Key Contributor to Atmospheric Aerosol, *Chem. Rev.*, 119, 3472–3509, <https://doi.org/10.1021/acs.chemrev.8b00395>, 2019.
- Bonn, B. and Moorgat, G. K.: New particle formation during  $\alpha$ - and  $\beta$ -pinene oxidation by O<sub>3</sub>, OH and NO<sub>3</sub>, and the influence of water vapour: particle size distribution studies, *Atmos. Chem. Phys.*, 2, 183–196, <https://doi.org/10.5194/acp-2-183-2002>, 2002.
- Chhantyal-Pun, R., Rotavera, B., McGillen, M. R., Khan, M. A. H., Eskola, A. J., Caravan, R. L., Blacker, L., Tew, D. P., Osborn, D. L., and Percival, C. J.: Criegee intermediate reactions with carboxylic acids: a potential source of secondary organic aerosol in the atmosphere, *ACS Earth and Space Chemistry*, 2, 833–842, 2018.
- Claeys, M., Iinuma, Y., Szmigielski, R., Surratt, J. D., Blockhuys, F., Van Alsenoy, C., Boege, O., Sierau, B., Gomez-Gonzalez, Y., Vermeylen, R., Van der Veken, P., Shahgholi, M., Chan, A. W. H., Herrmann, H., Seinfeld, J. H., and Maenhaut, W.: Terpenylic Acid and Related Compounds from the Oxidation of  $\alpha$ -Pinene: Implications for New Particle Formation and Growth above Forests, *Environ. Sci. Technol.*, 43, 6976–6982, <https://doi.org/10.1021/es9007596>, 2009.
- Clafin, M. S., Krechmer, J. E., Hu, W., Jimenez, J. L., and Ziemann, P. J.: Functional group composition of secondary organic aerosol formed from ozonolysis of  $\alpha$ -pinene under high VOC and autoxidation conditions, *ACS Earth and Space Chemistry*, 2, 1196–1210, 2018.
- Crouse, J. D., Nielsen, L. B., Jørgensen, S., Kjaergaard, H. G., and Wennberg, P. O.: Autoxidation of Organic Compounds

- in the Atmosphere, *The J. Phys. Chem. Lett.*, 4, 3513–3520, <https://doi.org/10.1021/jz4019207>, 2013.
- DeCarlo, P. F., Kimmel, J. R., Trimborn, A., Northway, M. J., Jayne, J. T., Aiken, A. C., Gonin, M., Fuhrer, K., Horvath, T., Docherty, K. S., Worsnop, D. R., and Jimenez, J. L.: Field-Deployable, High-Resolution, Time-of-Flight Aerosol Mass Spectrometer, *Anal. Chem.*, 78, 8281–8289, <https://doi.org/10.1021/ac061249n>, 2006.
- DePalma, J. W., Horan, A. J., Hall Iv, W. A., and Johnston, M. V.: Thermodynamics of oligomer formation: implications for secondary organic aerosol formation and reactivity, *Phys. Chem. Chem. Phys.*, 15, 6935–6944, <https://doi.org/10.1039/C3CP44586K>, 2013.
- Donahue, N. M., Henry, K. M., Mentel, T. F., Kiendler-Scharr, A., Spindler, C., Bohn, B., Brauers, T., Dorn, H. P., Fuchs, H., and Tillmann, R.: Aging of biogenic secondary organic aerosol via gas-phase OH radical reactions, *P. Natl. Acad. Sci. USA*, 109, 13503–13508, 2012a.
- Donahue, N. M., Kroll, J. H., Pandis, S. N., and Robinson, A. L.: A two-dimensional volatility basis set – Part 2: Diagnostics of organic-aerosol evolution, *Atmos. Chem. Phys.*, 12, 615–634, <https://doi.org/10.5194/acp-12-615-2012>, 2012b.
- Ehn, M., Thornton, J. A., Kleist, E., Sipilä, M., Junninen, H., Pullinen, I., Springer, M., Rubach, F., Tillmann, R., and Lee, B.: A large source of low-volatility secondary organic aerosol, *Nature*, 506, 476–479, <https://doi.org/10.1038/nature13032>, 2014.
- Ehn, M., Berndt, T., Wildt, J., and Mentel, T.: Highly Oxygenated Molecules from Atmospheric Autoxidation of Hydrocarbons: A Prominent Challenge for Chemical Kinetics Studies, *Int. J. Chem. Kinet.*, 49, 821–831, <https://doi.org/10.1002/kin.21130>, 2017.
- Elm, J.: Unexpected Growth Coordinate in Large Clusters Consisting of Sulfuric Acid and  $C_8H_{12}O_6$  Tricarboxylic Acid, *J. Phys. Chem. A*, 123, 3170–3175, <https://doi.org/10.1021/acs.jpca.9b00428>, 2019.
- Elm, J., Myllys, N., and Kurtén, T.: What Is Required for Highly Oxidized Molecules To Form Clusters with Sulfuric Acid?, *J. Phys. Chem. A*, 121, 4578–4587, <https://doi.org/10.1021/acs.jpca.7b03759>, 2017.
- Gao, S., Ng, N. L., Keywood, M., Varutbangkul, V., Bahreini, R., Nenes, A., He, J., Yoo, K. Y., Beauchamp, J., and Hodyss, R. P.: Particle phase acidity and oligomer formation in secondary organic aerosol, *Environ. Sci. Technol.*, 38, 6582–6589, 2004.
- Gao, Y., Hall, W. A., and Johnston, M. V.: Molecular Composition of Monoterpene Secondary Organic Aerosol at Low Mass Loading, *Environ. Sci. Technol.*, 44, 7897–7902, <https://doi.org/10.1021/es101861k>, 2010.
- Hakola, H., Tarvainen, V., Laurila, T., Hiltunen, V., Hellén, H., and Keronen, P.: Seasonal variation of VOC concentrations above a boreal coniferous forest, *Atmos. Environ.*, 37, 1623–1634, 2003.
- Hakola, H., Hellén, H., Tarvainen, V., Bäck, J., Patokoski, J., and Rinne, J.: Annual variations of atmospheric VOC concentrations in a boreal forest, *Boreal Environ. Res.*, 14, 722–730, 2009.
- Hoffmann, T., Bandur, R., Marggraf, U., and Linscheid, M.: Molecular composition of organic aerosols formed in the  $\alpha$ -pinene/O<sub>3</sub> reaction: Implications for new particle formation processes, *J. Geophys. Res.-Atmos.*, 103, 25569–25578, 1998.
- Huang, W., Saathoff, H., Pajunoja, A., Shen, X., Naumann, K.-H., Wagner, R., Virtanen, A., Leisner, T., and Mohr, C.:  $\alpha$ -Pinene secondary organic aerosol at low temperature: chemical composition and implications for particle viscosity, *Atmos. Chem. Phys.*, 18, 2883–2898, <https://doi.org/10.5194/acp-18-2883-2018>, 2018.
- Jensen, L. N., Canagaratna, M. R., Kristensen, K., Quéléver, L. L. J., Rosati, B., Teiwes, R., Glasius, M., Pedersen, H. B., Ehn, M., and Bilde, M.: Temperature and VOC concentration as controlling factors for chemical composition of alpha-pinene derived secondary organic aerosol, *Atmos. Chem. Phys. Discuss.*, <https://doi.org/10.5194/acp-2020-100>, in review, 2020.
- Jokinen, T., Sipilä, M., Junninen, H., Ehn, M., Lönn, G., Hakala, J., Petäjä, T., Mauldin III, R. L., Kulmala, M., and Worsnop, D. R.: Atmospheric sulphuric acid and neutral cluster measurements using CI-API-TOF, *Atmos. Chem. Phys.*, 12, 4117–4125, <https://doi.org/10.5194/acp-12-4117-2012>, 2012.
- Jokinen, T., Sipilä, M., Richters, S., Kerminen, V.-M., Paasonen, P., Stratmann, F., Worsnop, D., Kulmala, M., Ehn, M., Herrmann, H., and Berndt, T.: Rapid Autoxidation Forms Highly Oxidized RO<sub>2</sub> Radicals in the Atmosphere, *Angew. Chem. Int. Edit.*, 53, 14596–14600, <https://doi.org/10.1002/anie.201408566>, 2014.
- Jonsson, Å. M., Hallquist, M., and Ljungström, E.: The effect of temperature and water on secondary organic aerosol formation from ozonolysis of limonene,  $\Delta^3$ -carene and  $\alpha$ -pinene, *Atmos. Chem. Phys.*, 8, 6541–6549, <https://doi.org/10.5194/acp-8-6541-2008>, 2008.
- Junninen, H., Ehn, M., Petäjä, T., Luosujärvi, L., Kotiaho, T., Kostianinen, R., Rohner, U., Gonin, M., Fuhrer, K., Kulmala, M., and Worsnop, D. R.: A high-resolution mass spectrometer to measure atmospheric ion composition, *Atmos. Meas. Tech.*, 3, 1039–1053, <https://doi.org/10.5194/amt-3-1039-2010>, 2010.
- Kahnt, A., Vermeylen, R., Iinuma, Y., Safi Shalamzari, M., Maenhaut, W., and Claeys, M.: High-molecular-weight esters in  $\alpha$ -pinene ozonolysis secondary organic aerosol: structural characterization and mechanistic proposal for their formation from highly oxygenated molecules, *Atmos. Chem. Phys.*, 18, 8453–8467, <https://doi.org/10.5194/acp-18-8453-2018>, 2018.
- Kenseth, C. M., Huang, Y., Zhao, R., Dalleska, N. F., Hethcox, J. C., Stoltz, B. M., and Seinfeld, J. H.: Synergistic O<sub>3</sub> + OH oxidation pathway to extremely low-volatility dimers revealed in  $\beta$ -pinene secondary organic aerosol, *P. Natl. Acad. Sci. USA*, 115, 8301–8306, <https://doi.org/10.1073/pnas.1804671115>, 2018.
- Khan, M., Percival, C., Caravan, R., Taatjes, C., and Shallcross, D.: Criegee intermediates and their impacts on the troposphere, *Environ. Sci.-Proc. Imp.*, 20, 437–453, 2018.
- Kirkby, J., Duplissy, J., Sengupta, K., Frege, C., Gordon, H., Williamson, C., Heinritzi, M., Simon, M., Yan, C., Almeida, J., Tröstl, J., Nieminen, T., Ortega, I. K., Wagner, R., Adamov, A., Amorim, A., Bernhammer, A.-K., Bianchi, F., Breitenlechner, M., Brilke, S., Chen, X., Craven, J., Dias, A., Ehrhart, S., Flagan, R. C., Franchin, A., Fuchs, C., Guida, R., Hakala, J., Hoyle, C. R., Jokinen, T., Junninen, H., Kangasluoma, J., Kim, J., Krapf, M., Kürten, A., Laaksonen, A., Lehtipalo, J., Makhmutov, V., Mathot, S., Molteni, U., Onnela, A., Peräkylä, O., Piel, F., Petäjä, T., Praplan, A. P., Pringle, K., Rap, A., Richards, N. A. D., Riipinen, I., Rissanen, M. P., Rondo, L., Sarnela, N., Schobesberger, S., Scott, C. E., Seinfeld, J. H., Sipilä, M., Steiner, G., Stozhkov, Y., Stratmann, F., Tomé, A., Virtanen, A., Vogel, A. L., Wagner, A. C., Wagner, P. E., Weingartner, E., Wimmer, D., Winkler, P. M., Ye, P., Zhang, X., Hansel, A., Dommen, J., Donahue, N.

- M., Worsnop, D. R., Baltensperger, U., Kulmala, M., Carslaw, K. S., and Curtius, J.: Ion-induced nucleation of pure biogenic particles, *Nature*, 533, 521–526, <https://doi.org/10.1038/nature17953>, 2016.
- Kourtchev, I., Doussin, J.-F., Giorio, C., Mahon, B., Wilson, E. M., Maurin, N., Pangu, E., Venables, D. S., Wenger, J. C., and Kalberer, M.: Molecular composition of fresh and aged secondary organic aerosol from a mixture of biogenic volatile compounds: a high-resolution mass spectrometry study, *Atmos. Chem. Phys.*, 15, 5683–5695, <https://doi.org/10.5194/acp-15-5683-2015>, 2015.
- Kourtchev, I., Giorio, C., Manninen, A., Wilson, E., Mahon, B., Aalto, J., Kajos, M., Venables, D., Ruuskanen, T., and Levula, J.: Enhanced Volatile Organic Compounds emissions and organic aerosol mass increase the oligomer content of atmospheric aerosols, *Sci. Rep.*, 6, 35038, <https://doi.org/10.1038/srep35038>, 2016.
- Kristensen, K. and Glasius, M.: Organosulfates and oxidation products from biogenic hydrocarbons in fine aerosols from a forest in North West Europe during spring, *Atmos. Environ.*, 45, 4546–4556, 2011.
- Kristensen, K., Enggrob, K. L., King, S. M., Worton, D. R., Platt, S. M., Mortensen, R., Rosenoern, T., Surratt, J. D., Bilde, M., Goldstein, A. H., and Glasius, M.: Formation and occurrence of dimer esters of pinene oxidation products in atmospheric aerosols, *Atmos. Chem. Phys.*, 13, 3763–3776, <https://doi.org/10.5194/acp-13-3763-2013>, 2013.
- Kristensen, K., Cui, T., Zhang, H., Gold, A., Glasius, M., and Surratt, J. D.: Dimers in  $\alpha$ -pinene secondary organic aerosol: effect of hydroxyl radical, ozone, relative humidity and aerosol acidity, *Atmos. Chem. Phys.*, 14, 4201–4218, <https://doi.org/10.5194/acp-14-4201-2014>, 2014.
- Kristensen, K., Watne, Å. K., Hammes, J., Lutz, A., Petäjä, T., Hallquist, M., Bilde, M., and Glasius, M.: High-Molecular Weight Dimer Esters Are Major Products in Aerosols from  $\alpha$ -Pinene Ozonolysis and the Boreal Forest, *Environ. Sci. Tech. Lett.*, 3, 280–285, <https://doi.org/10.1021/acs.estlett.6b00152>, 2016.
- Kristensen, K., Jensen, L., Glasius, M., and Bilde, M.: The effect of sub-zero temperature on the formation and composition of secondary organic aerosol from ozonolysis of alpha-pinene, *Enviro. Sci.-Proc. Imp.*, 19, 1220–1234, 2017.
- Kroll, J. H. and Seinfeld, J. H.: Chemistry of secondary organic aerosol: Formation and evolution of low-volatility organics in the atmosphere, *Atmos. Environ.*, 42, 3593–3624, 2008.
- Kulmala, M., Kontkanen, J., Junninen, H., Lehtipalo, K., Manninen, H. E., Nieminen, T., Petäjä, T., Sipilä, M., Schobesberger, S., and Rantala, P.: Direct observations of atmospheric aerosol nucleation, *Science*, 339, 943–946, 2013.
- Kurtein, T., Tiusanen, K., Roldin, P., Rissanen, M., Luy, J.-N., Boy, M., Ehn, M., and Donahue, N.:  $\alpha$ -Pinene autoxidation products may not have extremely low saturation vapor pressures despite high O:C ratios, *J. Phys. Chem. A*, 120, 2569–2582, 2016.
- Lawler, M. J., Rissanen, M. P., Ehn, M., Mauldin III, R. L., Sarnela, N., Sipilä, M., and Smith, J. N.: Evidence for diverse biogeochemical drivers of boreal forest new particle formation, *Geophys. Res. Lett.*, 45, 2038–2046, 2018.
- Lee, B. H., D'Ambro, E. L., Lopez-Hilfiker, F. D., Schobesberger, S., Mohr, C., Zawadowicz, M. A., Liu, J., Shilling, J. E., Hu, W., Palm, B. B., Jimenez, J. L., Hao, L., Virtanen, A., Zhang, H., Goldstein, A. H., Pye, H. O. T., and Thornton, J. A.: Resolving Ambient Organic Aerosol Formation and Aging Pathways with Simultaneous Molecular Composition and Volatility Observations, *ACS Earth and Space Chemistry*, 4, 391–402, <https://doi.org/10.1021/acsearthspacechem.9b00302>, 2020.
- Lee, S. and Kamens, R. M.: Particle nucleation from the reaction of  $\alpha$ -pinene and O<sub>3</sub>, *Atmos. Environ.*, 39, 6822–6832, <https://doi.org/10.1016/j.atmosenv.2005.07.062>, 2005.
- Lee, S. H., Uin, J., Guenther, A. B., de Gouw, J. A., Yu, F., Nadykto, A. B., Herb, J., Ng, N. L., Koss, A., and Brune, W. H.: Isoprene suppression of new particle formation: Potential mechanisms and implications, *J. Geophys. Res.-Atmos.*, 121, 14621–14635, 2016.
- Li, Y. and Shiraiwa, M.: Timescales of secondary organic aerosols to reach equilibrium at various temperatures and relative humidities, *Atmos. Chem. Phys.*, 19, 5959–5971, <https://doi.org/10.5194/acp-19-5959-2019>, 2019.
- McGillen, M. R., Curchod, B. F., Chhantyal-Pun, R., Beames, J. M., Watson, N., Khan, M. A. H., McMahan, L., Shallcross, D. E., and Orr-Ewing, A. J.: Criegee intermediate–alcohol reactions, a potential source of functionalized hydroperoxides in the atmosphere, *ACS Earth and Space Chemistry*, 1, 664–672, 2017.
- Metzger, A., Verheggen, B., Dommen, J., Duplissy, J., Prevot, A. S., Weingartner, E., Riipinen, I., Kulmala, M., Spracklen, D. V., and Carslaw, K. S.: Evidence for the role of organics in aerosol particle formation under atmospheric conditions, *P. Natl. Acad. Sci. USA*, 107, 6646–6651, 2010.
- Mohr, C., Lopez-Hilfiker, F. D., Yli-Juuti, T., Heitto, A., Lutz, A., Hallquist, M., D'Ambro, E. L., Rissanen, M. P., Hao, L., and Schobesberger, S.: Ambient observations of dimers from terpene oxidation in the gas phase: Implications for new particle formation and growth, *Geophys. Res. Lett.*, 44, 2958–2966, 2017.
- Müller, L., Reinnig, M.-C., Naumann, K. H., Saathoff, H., Mentel, T. F., Donahue, N. M., and Hoffmann, T.: Formation of 3-methyl-1,2,3-butanetricarboxylic acid via gas phase oxidation of pinonic acid – a mass spectrometric study of SOA aging, *Atmos. Chem. Phys.*, 12, 1483–1496, <https://doi.org/10.5194/acp-12-1483-2012>, 2012.
- Mutzel, A., Poulain, L., Berndt, T., Iinuma, Y., Rodigast, M., Böge, O., Richters, S., Spindler, G., Sipilä, M., Jokinen, T., Kulmala, M., and Herrmann, H.: Highly Oxidized Multifunctional Organic Compounds Observed in Tropospheric Particles: A Field and Laboratory Study, *Environ. Sci. Technol.*, 49, 7754–7761, <https://doi.org/10.1021/acs.est.5b00885>, 2015.
- Nizkorodov, S. A., Laskin, J., and Laskin, A.: Molecular chemistry of organic aerosols through the application of high resolution mass spectrometry, *Phys. Chem. Chem. Phys.*, 13, 3612–3629, 2011.
- Noe, S. M., Hüve, K., Niinemets, Ü., and Copolovici, L.: Seasonal variation in vertical volatile compounds air concentrations within a remote hemiboreal mixed forest, *Atmos. Chem. Phys.*, 12, 3909–3926, <https://doi.org/10.5194/acp-12-3909-2012>, 2012.
- Noziere, B., Kalberer, M., Claeys, M., Allan, J., D'Anna, B., Decesari, S., Finessi, E., Glasius, M., Grgic, I., and Hamilton, J. F.: The molecular identification of organic compounds in the atmosphere: state of the art and challenges, *Chem. Rev.*, 115, 3919–3983, 2015.
- Pathak, R. K., Stanier, C. O., Donahue, N. M., and Pandis, S. N.: Ozonolysis of  $\alpha$ -pinene at atmospherically rele-

- vant concentrations: Temperature dependence of aerosol mass fractions (yields), *J. Geophys. Res.-Atmos.*, 112, D03201, <https://doi.org/10.1029/2006JD007436>, 2007.
- Peräkylä, O., Riva, M., Heikkinen, L., Quéléver, L., Roldin, P., and Ehn, M.: Experimental investigation into the volatilities of highly oxygenated organic molecules (HOMs), *Atmos. Chem. Phys.*, 20, 649–669, <https://doi.org/10.5194/acp-20-649-2020>, 2020.
- Quéléver, L. L. J., Kristensen, K., Normann Jensen, L., Rosati, B., Teiwes, R., Daellenbach, K. R., Peräkylä, O., Roldin, P., Bossi, R., Pedersen, H. B., Glasius, M., Bilde, M., and Ehn, M.: Effect of temperature on the formation of highly oxygenated organic molecules (HOMs) from alpha-pinene ozonolysis, *Atmos. Chem. Phys.*, 19, 7609–7625, <https://doi.org/10.5194/acp-19-7609-2019>, 2019.
- Renbaum-Wolff, L., Grayson, J. W., Bateman, A. P., Kuwata, M., Sellier, M., Murray, B. J., Shilling, J. E., Martin, S. T., and Bertram, A. K.: Viscosity of  $\alpha$ -pinene secondary organic material and implications for particle growth and reactivity, *P. Natl. Acad. Sci. USA*, 110, 8014–8019, <https://doi.org/10.1073/pnas.1219548110>, 2013.
- Riccobono, F., Schobesberger, S., Scott, C. E., Dommen, J., Ortega, I. K., Rondo, L., Almeida, J., Amorim, A., Bianchi, F., and Breitenlechner, M.: Oxidation products of biogenic emissions contribute to nucleation of atmospheric particles, *Science*, 344, 717–721, 2014.
- Rissanen, M. P., Kurtén, T., Sipilä, M., Thornton, J. A., Kausiala, O., Garmash, O., Kjaergaard, H. G., Petäjä, T., Worsnop, D. R., Ehn, M., and Kulmala, M.: Effects of Chemical Complexity on the Autoxidation Mechanisms of Endocyclic Alkene Ozonolysis Products: From Methylcyclohexenes toward Understanding  $\alpha$ -Pinene, *J. Phys. Chem. A*, 119, 4633–4650, <https://doi.org/10.1021/jp510966g>, 2015.
- Rosati, B., Teiwes, R., Kristensen, K., Bossi, R., Skov, H., Glasius, M., Pedersen, H. B., and Bilde, M.: Factor analysis of chemical ionization experiments: Numerical simulations and an experimental case study of the ozonolysis of  $\alpha$ -pinene using a PTR-ToF-MS, *Atmos. Environ.*, 199, 15–31, <https://doi.org/10.1016/j.atmosenv.2018.11.012>, 2019.
- Saathoff, H., Naumann, K.-H., Möhler, O., Jonsson, Å. M., Hallquist, M., Kiendler-Scharr, A., Mentel, Th. F., Tillmann, R., and Schurath, U.: Temperature dependence of yields of secondary organic aerosols from the ozonolysis of  $\alpha$ -pinene and limonene, *Atmos. Chem. Phys.*, 9, 1551–1577, <https://doi.org/10.5194/acp-9-1551-2009>, 2009.
- Shiraiwa, M. and Seinfeld, J. H.: Equilibration timescale of atmospheric secondary organic aerosol partitioning, *Geophys. Res. Lett.*, 39, L24801, <https://doi.org/10.1029/2012GL054008>, 2012.
- Simon, M., Dada, L., Heinritzi, M., Scholz, W., Stolzenburg, D., Fischer, L., Wagner, A. C., Kürten, A., Rörup, B., He, X.-C., Almeida, J., Baalbaki, R., Baccarini, A., Bauer, P. S., Beck, L., Bergen, A., Bianchi, F., Bräkling, S., Brilke, S., Caudillo, L., Chen, D., Chu, B., Dias, A., Draper, D. C., Duplissy, J., El-Haddad, I., Finkenzeller, H., Frege, C., Gonzalez-Carracedo, L., Gordon, H., Granzin, M., Hakala, J., Hofbauer, V., Hoyle, C. R., Kim, C., Kong, W., Lamkaddam, H., Lee, C. P., Lehtipalo, K., Leiminger, M., Mai, H., Manninen, H. E., Marie, G., Marten, R., Mentler, B., Molteni, U., Nichman, L., Nie, W., Ojdanic, A., Onnela, A., Partoll, E., Petäjä, T., Pfeifer, J., Philippov, M., Quéléver, L. L. J., Ranjithkumar, A., Rissanen, M. P., Schallhart, S., Schobesberger, S., Schuchmann, S., Shen, J., Sipilä, M., Steiner, G., Stozhkov, Y., Tauber, C., Tham, Y. J., Tomé, A. R., Vazquez-Pufleau, M., Vogel, A. L., Wagner, R., Wang, M., Wang, D. S., Wang, Y., Weber, S. K., Wu, Y., Xiao, M., Yan, C., Ye, P., Ye, Q., Zauner-Wieczorek, M., Zhou, X., Baltensperger, U., Dommen, J., Flagan, R. C., Hansel, A., Kulmala, M., Volkamer, R., Winkler, P. M., Worsnop, D. R., Donahue, N. M., Kirkby, J., and Curtius, J.: Molecular understanding of new-particle formation from  $\alpha$ -pinene between  $-50$  and  $+25$  °C, *Atmos. Chem. Phys.*, 20, 9183–9207, <https://doi.org/10.5194/acp-20-9183-2020>, 2020.
- Sindelarova, K., Granier, C., Bouarar, I., Guenther, A., Tilmes, S., Stavrou, T., Müller, J.-F., Kuhn, U., Stefani, P., and Knorr, W.: Global data set of biogenic VOC emissions calculated by the MEGAN model over the last 30 years, *Atmos. Chem. Phys.*, 14, 9317–9341, <https://doi.org/10.5194/acp-14-9317-2014>, 2014.
- Stolzenburg, D., Fischer, L., Vogel, A. L., Heinritzi, M., Schervish, M., Simon, M., Wagner, A. C., Dada, L., Ahonen, L. R., Amorim, A., Baccarini, A., Bauer, P. S., Baumgartner, B., Bergen, A., Bianchi, F., Breitenlechner, M., Brilke, S., Buenrostro Mazon, S., Chen, D., Dias, A., Draper, D. C., Duplissy, J., El Haddad, I., Finkenzeller, H., Frege, C., Fuchs, C., Garmash, O., Gordon, H., He, X., Helm, J., Hofbauer, V., Hoyle, C. R., Kim, C., Kirkby, J., Kontkanen, J., Kürten, A., Lampilahti, J., Lawler, M., Lehtipalo, K., Leiminger, M., Mai, H., Mathot, S., Mentler, B., Molteni, U., Nie, W., Nieminen, T., Nowak, J. B., Ojdanic, A., Onnela, A., Passananti, M., Petäjä, T., Quéléver, L. L. J., Rissanen, M. P., Sarnela, N., Schallhart, S., Tauber, C., Tomé, A., Wagner, R., Wang, M., Weitz, L., Wimmer, D., Xiao, M., Yan, C., Ye, P., Zha, Q., Baltensperger, U., Curtius, J., Dommen, J., Flagan, R. C., Kulmala, M., Smith, J. N., Worsnop, D. R., Hansel, A., Donahue, N. M., and Winkler, P. M.: Rapid growth of organic aerosol nanoparticles over a wide tropospheric temperature range, *P. Natl. Acad. Sci. USA*, 115, 9122–9127, <https://doi.org/10.1073/pnas.1807604115>, 2018.
- Svendby, T. M., Lazaridis, M., and Tørseth, K.: Temperature dependent secondary organic aerosol formation from terpenes and aromatics, *J. Atmos. Chem.*, 59, 25–46, <https://doi.org/10.1007/s10874-007-9093-7>, 2008.
- Szmigielski, R., Surratt, J. D., Gómez-González, Y., Van der Veken, P., Kourtchev, I., Vermeulen, R., Blockhuys, F., Jaoui, M., Kleindienst, T. E., and Lewandowski, M.: 3-methyl-1, 2, 3-butanetricarboxylic acid: An atmospheric tracer for terpene secondary organic aerosol, *Geophys. Res. Lett.*, 34, L24811, <https://doi.org/10.1029/2007GL031338>, 2007.
- Tillmann, R., Hallquist, M., Jonsson, Å. M., Kiendler-Scharr, A., Saathoff, H., Iinuma, Y., and Mentel, Th. F.: Influence of relative humidity and temperature on the production of pinonaldehyde and OH radicals from the ozonolysis of  $\alpha$ -pinene, *Atmos. Chem. Phys.*, 10, 7057–7072, <https://doi.org/10.5194/acp-10-7057-2010>, 2010.
- Tolocka, M. P., Jang, M., Ginter, J. M., Cox, F. J., Kamens, R. M., and Johnston, M. V.: Formation of Oligomers in Secondary Organic Aerosol, *Environ. Sci. Technol.*, 38, 1428–1434, <https://doi.org/10.1021/es035030r>, 2004.
- Tolocka, M. P., Heaton, K. J., Dreyfus, M. A., Wang, S., Zordan, C. A., Saul, T. D., and Johnston, M. V.: Chemistry of Particle Inception and Growth during  $\alpha$ -Pinene Ozonolysis, *Environ. Sci.*

- Technol., 40, 1843–1848, <https://doi.org/10.1021/es051926f>, 2006.
- Tröstl, J., Chuang, W. K., Gordon, H., Heinritzi, M., Yan, C., Molteni, U., Ahlm, L., Frege, C., Bianchi, F., and Wagner, R.: The role of low-volatility organic compounds in initial particle growth in the atmosphere, *Nature*, 533, 527–531, <https://doi.org/10.1038/nature18271> 2016.
- Vanhanen, J., Mikkilä, J., Lehtipalo, K., Sipilä, M., Manninen, H. E., Siivola, E., Petäjä, T., and Kulmala, M.: Particle Size Magnifier for Nano-CN Detection, *Aerosol Sci. Tech.*, 45, 533–542, <https://doi.org/10.1080/02786826.2010.547889>, 2011.
- Vereecken, L., Müller, J.-F., and Peeters, J.: Low-volatility poly-oxygenates in the OH-initiated atmospheric oxidation of  $\alpha$ -pinene: impact of non-traditional peroxy radical chemistry, *Phys. Chem. Chem. Phys.*, 9, 5241–5248, 2007.
- von Hessberg, C., von Hessberg, P., Pöschl, U., Bilde, M., Nielsen, O. J., and Moortgat, G. K.: Temperature and humidity dependence of secondary organic aerosol yield from the ozonolysis of  $\beta$ -pinene, *Atmos. Chem. Phys.*, 9, 3583–3599, <https://doi.org/10.5194/acp-9-3583-2009>, 2009.
- Warren, B., Austin, R. L., and Cocker, D. R.: Temperature dependence of secondary organic aerosol, *Atmos. Environ.*, 43, 3548–3555, <https://doi.org/10.1016/j.atmosenv.2009.04.011>, 2009.
- Witkowski, B. and Gierczak, T.: Early stage composition of SOA produced by  $\alpha$ -pinene/ozone reaction:  $\alpha$ -Acyloxyhydroperoxy aldehydes and acidic dimers, *Atmos. Environ.*, 95, 59–70, 2014.
- Yasmeen, F., Vermeylen, R., Szmigielski, R., Iinuma, Y., Böge, O., Herrmann, H., Maenhaut, W., and Claeys, M.: Terpenylic acid and related compounds: precursors for dimers in secondary organic aerosol from the ozonolysis of  $\alpha$ - and  $\beta$ -pinene, *Atmos. Chem. Phys.*, 10, 9383–9392, <https://doi.org/10.5194/acp-10-9383-2010>, 2010.
- Zaveri, R. A., Easter, R. C., Shilling, J. E., and Seinfeld, J. H.: Modeling kinetic partitioning of secondary organic aerosol and size distribution dynamics: representing effects of volatility, phase state, and particle-phase reaction, *Atmos. Chem. Phys.*, 14, 5153–5181, <https://doi.org/10.5194/acp-14-5153-2014>, 2014.
- Zaveri, R. A., Shilling, J. E., Zelenyuk, A., Zawadowicz, M. A., Suski, K., China, S., Bell, D. M., Veghte, D., and Laskin, A.: Particle-Phase Diffusion Modulates Partitioning of Semivolatile Organic Compounds to Aged Secondary Organic Aerosol, *Environ. Sci. Technol.*, 54, 2595–2605, <https://doi.org/10.1021/acs.est.9b05514>, 2020.
- Zhang, H., Yee, L. D., Lee, B. H., Curtis, M. P., Worton, D. R., Isaacman-VanWertz, G., Offenberg, J. H., Lewandowski, M., Kleindienst, T. E., and Beaver, M. R.: Monoterpenes are the largest source of summertime organic aerosol in the southeastern United States, *P. Natl. Acad. Sci. USA*, 115, 2038–2043, 2018.
- Zhang, X., McVay, R. C., Huang, D. D., Dalleska, N. F., Aumont, B., Flagan, R. C., and Seinfeld, J. H.: Formation and evolution of molecular products in  $\alpha$ -pinene secondary organic aerosol, *P. Natl. Acad. Sci. USA*, 112, 14168–14173, 2015.
- Zhang, X., Lambe, A. T., Upshur, M. A., Brooks, W. A., Gray Beï, A., Thomson, R. J., Geiger, F. M., Surratt, J. D., Zhang, Z., and Gold, A.: Highly oxygenated multifunctional compounds in  $\alpha$ -pinene secondary organic aerosol, *Environ. Sci. Technol.*, 51, 5932–5940, 2017.
- Zhao, R., Kenseth, C. M., Huang, Y., Dalleska, N. F., Kuang, X. M., Chen, J., Paulson, S. E., and Seinfeld, J. H.: Rapid Aqueous-Phase Hydrolysis of Ester Hydroperoxides Arising from Criegee Intermediates and Organic Acids, *J. Phys. Chem. A*, 122, 5190–5201, 2018a.
- Zhao, Y., Wingen, L. M., Perraud, V., Greaves, J., and Finlayson-Pitts, B. J.: Role of the reaction of stabilized Criegee intermediates with peroxy radicals in particle formation and growth in air, *Phys. Chem. Chem. Phys.*, 17, 12500–12514, 2015.
- Zhao, Y., Thornton, J. A., and Pye, H. O.: Quantitative constraints on autoxidation and dimer formation from direct probing of monoterpene-derived peroxy radical chemistry, *P. Natl. Acad. Sci. USA*, 115, 12142–12147, 2018b.
- Zhao, Z., Le, C., Xu, Q., Peng, W., Jiang, H., Lin, Y.-H., Cocker, D. R., and Zhang, H.: Compositional Evolution of Secondary Organic Aerosol as Temperature and Relative Humidity Cycle in Atmospherically Relevant Ranges, *ACS Earth and Space Chemistry*, 3, 2549–2558, <https://doi.org/10.1021/acsearthspacechem.9b00232>, 2019a.
- Zhao, Z., Tolentino, R., Lee, J., Vuong, A., Yang, X., and Zhang, H.: Interfacial dimerization by organic radical reactions during heterogeneous oxidative aging of oxygenated organic aerosols, *J. Phys. Chem. A*, 123, 10782–10792, 2019b.